

# Resiliency and Reliability Planning of the Electric Grid in Natural Disaster Affected Areas

by

Marc Barbar

Submitted to the Department of Electrical Engineering and Computer Science

in partial fulfillment of the requirements for the degree of

Masters of Science in Electrical Engineering and Computer Science

at the

MASSACHUSETTS INSTITUTE OF TECHNOLOGY

June 2019

© Massachusetts Institute of Technology 2019. All rights reserved.

Author .....  
Department of Electrical Engineering and Computer Science  
May 23, 2019

Certified by .....  
Dr. Jose Ignacio Pérez-Arriaga  
Visiting Professor, Sloan School of Management  
Professor, Electrical Engineering, Comillas University  
Thesis Supervisor

Accepted by .....  
Dr. Leslie A. Kolodziejcki  
Professor of Electrical Engineering and Computer Science  
Chair, Department Committee on Graduate Students





# Resiliency and Reliability Planning of the Electric Grid in Natural Disaster Affected Areas

by

Marc Barbar

Submitted to the Department of Electrical Engineering and Computer Science  
on May 23, 2019, in partial fulfillment of the  
requirements for the degree of  
Masters of Science in Electrical Engineering and Computer Science

## Abstract

The recent spike in the frequency of hurricanes in Central America has severely damaged the conventional electrical grid. Notably, the government of Puerto Rico laid out a plan to reinvent its energy sector to improve its level of resiliency against natural disasters. Better planning and preparation can minimize the damage that needs to be repaired on time. For instance, when necessary facilities, such as hospitals, lose access to electricity, the ability to manage a displaced population after a hurricane is diminished.

Computational planning tools allow policymakers and planners to take reliability metrics, resource constraints, interactions between off-grid and traditional grid-extension projects into account when designing contingency plans for the electric grid. The goal of this thesis is to explore the role of a hybrid decentralized structure of the electrical grid to improve the level of reliability through extraordinary circumstances.

In this thesis, I develop algorithms that are shown via several case studies. Given the proper input data, these algorithms can provide insight into the technical feasibility of where to deploy microgrids given the existing infrastructure. This research emphasizes the need for granular spatial data at the distribution level to make better planning decisions.

Thesis Supervisor: Dr. Jose Ignacio Pérez-Arriaga  
Title: Visiting Professor, Sloan School of Management  
Professor, Electrical Engineering, Comillas University



# Acknowledgments

Firstly, thank you to my advisor and thesis supervisor, Professor Jose Ignacio Perez-Arriaga, who provided the opportunity to get involved with this exciting and important project. His guidance and support pushed me to learn more, and his wealth of knowledge and experience challenged me to produce better results and make better use of my time at MIT. Overall it was much fun being his student.

Thank you to the Universal Access Lab team, particularly Dr. Carlos Mateo Domingo and Dr. Fernando de Cuadra who eased access and support to their Reference Network Models. Moreover, I am thankful for the time and feedback they regularly provided on my work.

Thank you, Dr. Pablo Duenas Martinez, for being supportive, willing to review my work, and be hands-on in assisting me with any question I had.

Thank you to the EECS Department for providing me with the unique opportunity of being at MIT to learn a new set of skills to make the world a better place.

Thank you to the team at Meteoblue based in Basel, Switzerland for providing free access to weather data for Puerto Rico.

A special thank you to my partner, Anna-Sophia Haub for being supportive and a sounding board anytime I had problems or concerns.

Last but not least, thank you to my father Fadi, mother Shamma and sister Julia for being a loving family, even from far away. I would not be here without you.

THIS PAGE INTENTIONALLY LEFT BLANK

# Contents

<b>1</b>	<b>Introduction</b>	<b>17</b>
1.1	Background and Motivation . . . . .	17
1.2	Research Questions . . . . .	18
1.3	Preview . . . . .	19
<b>2</b>	<b>Input Data Processing</b>	<b>21</b>
2.1	Overview of Input Data Processing . . . . .	21
2.2	Electric Grid . . . . .	22
2.2.1	Generation . . . . .	22
2.2.2	Substations . . . . .	22
2.2.3	Network Lines . . . . .	23
2.3	Building Demand . . . . .	25
2.4	Distribution Network . . . . .	27
2.4.1	Simplification . . . . .	28
2.4.2	Polygon to Centerline . . . . .	29
<b>3</b>	<b>Critical Infrastructure</b>	<b>31</b>
3.1	Critical Demand . . . . .	31
3.1.1	Load Profiles . . . . .	32
3.2	Critical Lines . . . . .	34
3.2.1	Steiner Tree . . . . .	34
3.2.2	Triangulation . . . . .	35
3.2.3	Algorithm . . . . .	37

<b>4</b>	<b>Microgrid Design</b>	<b>39</b>
4.1	Overview of Microgrid Design . . . . .	39
4.2	Microgrid Components . . . . .	40
4.2.1	Solar Panels and Battery Storage . . . . .	41
4.2.2	Diesel Generator . . . . .	41
4.3	Critical Operation . . . . .	42
4.3.1	Transportation Cost . . . . .	42
4.3.2	Demand Mix . . . . .	43
4.4	Modeling Components . . . . .	44
4.4.1	Parameters . . . . .	44
4.4.2	Variables . . . . .	46
4.4.3	Objective Function . . . . .	47
4.4.4	Constraints . . . . .	47
4.5	Results . . . . .	50
4.5.1	Case Results . . . . .	50
4.5.2	Library of Microgrids . . . . .	51
<b>5</b>	<b>Network Reliability</b>	<b>53</b>
5.1	Overview of Reliability . . . . .	53
5.2	Distance Metrics . . . . .	54
5.2.1	Segmentation . . . . .	54
5.2.2	Clustering . . . . .	55
5.3	Failure Rate . . . . .	59
5.3.1	Line Types . . . . .	59
5.3.2	Equipment Failure . . . . .	60
5.3.3	Node Reliability . . . . .	62
5.4	Reliability . . . . .	63
5.4.1	Top-Down Approach . . . . .	64
5.4.2	Bottom-Up Approach . . . . .	65
5.5	Multi-objective Optimization (MOO) . . . . .	66

5.5.1	Priority List . . . . .	68
5.5.2	Case Results . . . . .	69
<b>6</b>	<b>Network Hardening</b>	<b>71</b>
6.1	Overview of Network Hardening . . . . .	71
6.2	Upstream Hardening Decision . . . . .	72
6.2.1	Off-Grid Cost . . . . .	73
6.2.2	Grid Connection Cost . . . . .	73
6.3	Cost Allocation . . . . .	74
6.3.1	Decision Tree Algorithm: Case Example . . . . .	77
6.3.2	Solution . . . . .	81
6.3.3	Top-down observation . . . . .	83
6.3.4	Reliability Metrics . . . . .	84
6.4	Case Study . . . . .	84
<b>7</b>	<b>Summary, Discussion, and Conclusions</b>	<b>89</b>
7.1	Future Work . . . . .	90
<b>A</b>	<b>Tables</b>	<b>93</b>
<b>B</b>	<b>Code</b>	<b>97</b>
B.1	Steiner Tree Algorithm . . . . .	97
B.2	Clustering Algorithm . . . . .	98

THIS PAGE INTENTIONALLY LEFT BLANK



# List of Figures

2-1	Puerto Rico electricity generation map . . . . .	22
2-2	Puerto Rico MV/LV and HV/LV substations . . . . .	22
2-3	Photo: Erika P. Rodriguez . . . . .	23
2-4	Puerto Rico Transmission Network . . . . .	24
2-5	Puerto Rico HV Network . . . . .	24
2-6	Puerto Rico MV Network . . . . .	25
2-7	Urban Primary Distribution Network . . . . .	25
2-8	Rural Primary Distribution Network . . . . .	25
2-9	Building location with height information . . . . .	26
2-10	U.S. climate regions by county (Department of Energy) . . . . .	27
2-11	Section of primary distribution network in the city of San Juan . . . . .	28
2-12	Fixed distance buffer of distribution lines in the city of San Juan . . . . .	29
2-13	Polygon to center line workflow . . . . .	30
2-14	Center line of buffer . . . . .	30
3-1	Location of critical infrastructure in Puerto Rico . . . . .	32
3-2	Normalized 3 day residential demand profile from Key West, FL . . . . .	33
3-3	Normalized 3 day commercial demand profile from Key West, FL . . . . .	33
3-4	Normalized 3 day infrastructure demand profile from Key West, FL . . . . .	33
3-5	Simplified primary distribution network of the city of San Juan . . . . .	34
3-6	Downtown San Juan: Critical Loads (Stars), Substation (Triangle) . . . . .	34
3-7		35
3-8	Network nodes of Downtown San Juan . . . . .	36

3-9	Delaunay triangulation of nodes . . . . .	36
3-10	Triangulation results for Downtown San Juan . . . . .	37
3-11	Intermediate results: critical path of Downtown San Juan . . . . .	38
3-12	Final results: critical lines of Downtown San Juan . . . . .	38
4-1	Microgrid Topology . . . . .	40
4-2	Hurricane Season . . . . .	42
4-3	Urban San Juan: energy dispatch for 50 kW microgrid . . . . .	50
4-4	Rural San Juan: energy dispatch for 50 kW microgrid . . . . .	51
5-1	Critical infrastrcuture for the village of Orocovis . . . . .	54
5-2	Clustering Example: Case 1 . . . . .	56
5-3	Clustering Example: Case 2 . . . . .	57
5-4	Isleta de San Juan cluster of microgrids . . . . .	58
5-5	Electric System Islands Identified. Source: PREPA Recovery and System Resiliency Roadmap . . . . .	58
5-6	Sample Graph . . . . .	59
5-7	Sample network . . . . .	64
5-8	Top down reliability approach for the sample network from figure 5-7	65
5-9	Bottom up reliability approach for the sample network from figure 5-7	66
5-10	2 Dimensional Pareto Optimal Set . . . . .	67
5-11	Result LV and MV network of reliability model for Old San Juan . . .	69
5-12	Plot of 110 options of Old San Juan . . . . .	69
5-13	Result LV and MV network of reliability model for Orocovis . . . . .	70
6-1	Cost Allocation Example Network . . . . .	75
6-2	Cost Allocation Example: Combination 1 . . . . .	75
6-3	Cost Allocation Example: Combination 2 . . . . .	76
6-4	Cost Allocation Example: Combination 3 . . . . .	76
6-5	Cost Allocation Example: Combination 1 Off-grid MV Filtering . . .	77
6-6	Cost Allocation Example: Combination 3 Off-grid MV Filtering . . .	78

6-7	Cost Allocation Example: Combination 1 Off-grid MV Folding . . . .	78
6-8	Cost Allocation Example: Combination 3 Off-grid MV Folding . . . .	78
6-9	Cost Allocation Example: Combination 1 Off-grid MV Decision . . . .	79
6-10	Cost Allocation Example: Combination 3 Off-grid MV Decision . . . .	80
6-11	Cost Allocation Example: Combination 1 Off-grid HV MSP . . . . .	80
6-12	Cost Allocation Example: Combination 3 Off-grid HV MSP . . . . .	81
6-13	Cost Allocation Example: Combination 1 Off-grid HV Solution . . . .	82
6-14	Cost Allocation Example: Combination 3 Off-grid HV Solution . . . .	82
6-15	MV/LV Transformer location . . . . .	85
6-16	MV Steiner Tree . . . . .	85
6-17	MV Network post segmentation . . . . .	85
6-18	Line lengths of HV network . . . . .	86
6-19	Aggregated estimated demand at HV/MV stations in Millions of kilowatt- hours . . . . .	86
6-20	Solution for the San Juan and neighboring states . . . . .	87

THIS PAGE INTENTIONALLY LEFT BLANK

# List of Tables

5.1	Failure rate of underground equipment (per year value) . . . . .	60
A.1	Diesel generator investment cost bracket . . . . .	93
A.2	Generation facilities of Puerto Rico . . . . .	94
A.3	Diesel fuel transportation cost to rural territories . . . . .	95
A.4	Diesel fuel transportation cost to urban territories . . . . .	95

THIS PAGE INTENTIONALLY LEFT BLANK

# Chapter 1

## Introduction

### 1.1 Background and Motivation

Natural disasters, such as hurricane Maria that struck the island of Puerto Rico on September 16, 2017, can severely damage the electrical grid. It was not until July 9, 2018, that 98% of power was restored on the island. On August 28, 2018, the government revised the death tolls to a total of over 3,000 with several kilometers of transmission lines damaged and distribution networks destroyed [21]. While hurricane Harvey had a similar impact to Maria, 103 people died due to storm-related incidents. Restoration of service and recovery from the hurricane in Houston was rapid, which can be partly attributed to more advanced infrastructure. It is evident that natural disasters in low-income communities have disproportionate effects due to poor infrastructure and lack of resiliency. A noticeably rising frequency of hurricanes, especially in the Atlantic, stresses the need to address the problem of vulnerable electrical infrastructure.

As the electrical grid is today, electrical wires need to connect generation sources to loads through several voltage levels, stations, and elements. Overhead cables are the most vulnerable components when storms or hurricanes hit an area. Conversion from overhead electric systems to underground is the first solution brought to mind based on "out of sight out of mind." Undergrounding electrical networks are several times more expensive than traditional overhead wires and poles, but sometimes the

need for extra reliability or resilience, or just technical reasons justify the use of underground electrical infrastructure. It must be noted, that rainfall and floods are common effects of hurricanes, and simple undergrounding of the network based on a cost-benefit analysis can have undesirable consequences and cost associated with fixing or replacing underground wires. Moreover, underground cables are both more expensive and take longer time to install and maintain than overhead wires, due to access restrictions.

The quality of the output of this research is data dependent. Distribution companies seldom share network data for various reasons, making it challenging to produce proper studies that could contribute to the improvement of the sector. Open-source data is usually not accurate and outdated, but it serves as a starting point to validate the importance of creating power system data sets.

While rebuilding the same infrastructure is a short-term solution, it provides no long term benefit in hurricane-prone locations. Communities can find themselves with damaged infrastructure on a more frequent basis. This begs the need to find a new network topology and optimal hardening of the network via underground or reinforced wires and resilient generation while enforcing strong reliability constraints.

## 1.2 Research Questions

The MIT/Comillas Universal Access Lab has developed the state-of-the-art computational tool Rural Electrification Model (REM) that designs an optimal electrification plan in rural and developing areas through the deployment of minigrids, standalone systems, or extension of the grid [10]. REM makes several scientific assumptions and simplifications to account for the complexities of rural electrification. REM assumes no existing infrastructure and plans the network in greenfield mode. In this thesis, I will make use of different clustering algorithms in brownfield mode<sup>1</sup> to take into account the existing electrical grid. Quantifiable reliability measures are also taken into consideration for resiliency planning.

---

<sup>1</sup>Brownfield: using an existing network as the starting point of analysis



The central problem I will address in this thesis is *the development of computer-based tools that, based on the existing electrical infrastructure, design a more resilient and reliable network in areas prone to hurricanes and heavy storms*. This problem can be broken down into individual questions that will be answered throughout the thesis:

1. Which parts of the existing distribution network<sup>2</sup> must be hardened to meet prescribed reliability and resiliency standards?
2. Using REM's clustering algorithm, how can the deployment of microgrids in urban and rural areas improve the reliability of the overall network?
3. Which parts (if any) of the High Voltage electrical grid must be hardened and which generation — connected to this grid — must be maintained for long term reliable operation and cost savings?

## 1.3 Preview

A novel grid structure of microgrids and grid extension mix is proposed which provides resiliency to the grid and sustains the critical infrastructure immediately after a disaster.

Chapter 2 focuses on the replication of the existing grid and its parameters with a certain level of ambiguity and generalization, given that no accurate data has been provided. From the resulting data, the network triangulation and network optimization algorithms in chapter 3 are applied to identify and harden the critical network lines that reach the critical demand. This will segment the grid into critical microgrids. Chapter 4 designs the optimal energy dispatch and investment needed for each critical microgrid using linear programming optimization. Chapter 5 implements clustering algorithms inspired from REM to aggregate microgrids for cost minimization with reliability constraints. The tree solution from chapter 3 does not guarantee

---

<sup>2</sup>Distribution is defined by the medium voltage and primary low voltage networks. Sub-transmission is defined as high voltage distribution networks.

the reliability of the critical load; therefore, additional top-down and bottom-up algorithms are applied to produce reliable microgrids. Finally, chapter 6 takes into consideration the existing High Voltage network, and a cost minimization mix of microgrids and grid-extension is found to complete the overall electrical grid layout that meets strong reliability and resilience criteria under hurricane conditions.

# Chapter 2

## Input Data Processing

### 2.1 Overview of Input Data Processing

Research results heavily depend on the quality of input data. This is primarily why a lot of time and effort is being put in data collection, image processing, and quality control. However, this is not the primary purpose of this thesis. In this research, a method is proposed for deploying microgrids and their integration in the existing network, where the output is as impressive as the input data. Given that the government of Puerto Rico is undergoing significant changes in its structure and that PREPA<sup>1</sup> is bankrupt with overwhelming pointers to corruption, there has been a lack of communication and willingness to share data. The data used in this thesis has been either gathered from open sources [1] or developed internally.

The input data this research is mainly concerned with is the electrical network at different voltage levels, energy demand, substation location at different voltage levels and generation location and capacity. Some data will appear to be more crucial and sensitive to the output than, which will become evident throughout the development of the thesis.

---

<sup>1</sup>Puerto Rico Electric Power Authority

## 2.2 Electric Grid

First, careful attention must be given to the existing network to understand what currently exists and what are the degrees of freedom that can be used to reach an acceptable solution.

### 2.2.1 Generation

Figure 2-1 shows the location of existing generation facilities of Puerto Rico [14]. *(More information available on generation in table A.2 in the Appendix)*



Figure 2-1: Puerto Rico electricity generation map

### 2.2.2 Substations

Substations connected to the low voltage side or primary distribution transformers will be considered as the connection point of their allocated demand. They will serve as the center point for interconnection as shown in figure 2-2.

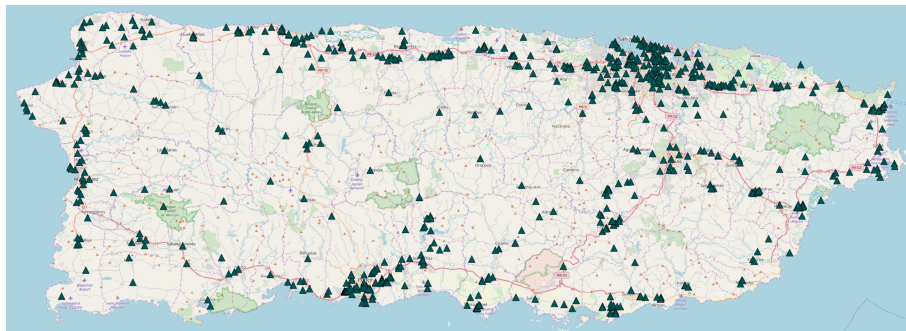


Figure 2-2: Puerto Rico MV/LV and HV/LV substations

### 2.2.3 Network Lines

Network topology serves as a constraint to the optimization of connecting and hardening lines that connect critical demand to both off-grid generation and main grid generation. The presented network in figures 2-4 to 2-6 is for Puerto Rico particularly.

The electric grid of Puerto Rico sustained many damages that, for the most part, have been addressed and thus the grid restored. However, this introduces resiliency and reliability concerns, which are the focus of this research. As seen in figure 2-3, the transmission tower was destroyed, which had a significant impact on the grid. This shows the vulnerability of overhead lines crossing areas difficult to reach, especially after a hurricane.



Figure 2-3: Photo: Erika P. Rodriguez

#### **Transmission: 230 kV**

The highly meshed network connects large generation to transmission substations. The wires are overhead suspended on large transmission towers, crossing rural areas often difficult to reach.



Figure 2-4: Puerto Rico Transmission Network

**High Voltage: 115 kV**

This network is strongly meshed at the core with radial branches connecting some generation facilities and transmission substations to HV/MV substations. Occasionally the high voltage network is directly connected to the low voltage side through high voltage to low voltage transformers. The wires are also overhead.

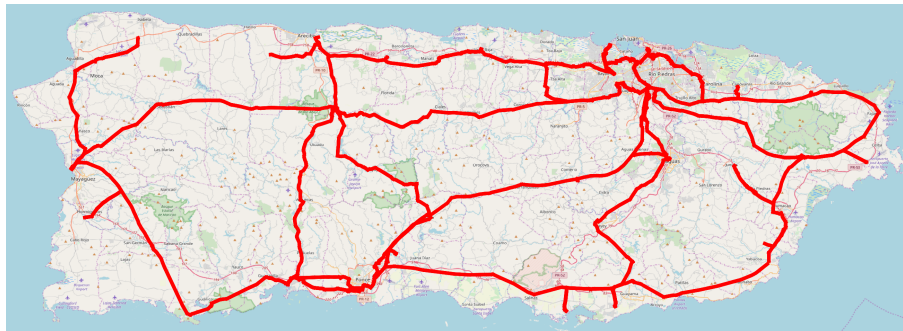


Figure 2-5: Puerto Rico HV Network

**Medium Voltage: 38 kV**

Radial network with select meshed features connects small generation and HV/MV substations to primary distribution transformers. The wires are overhead in rural and para-urban areas, but underground in urban areas.

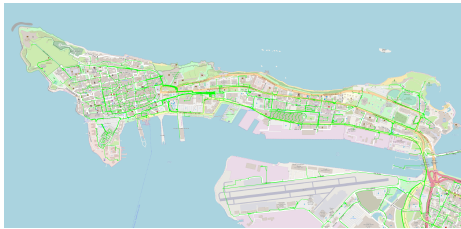
**Low Voltage - Primary Distribution: 7.6 kV and below**

Radial network starting from the medium voltage to low voltage substations, even though radial reliability measures require the addition of electric switches to change



Figure 2-6: Puerto Rico MV Network

the network configuration if fault occurs on the system. Such measures are accounted for as simplified loops as presented in Chapter 3.

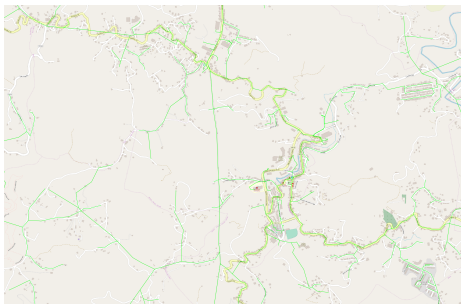


(a) City of San Juan



(b) Urban LV Network

Figure 2-7: Urban Primary Distribution Network



(a) Town of Orocovis



(b) Rural LV Network

Figure 2-8: Rural Primary Distribution Network

## 2.3 Building Demand

Given building shapes as shown in figure 2-9 and their height data, the demand of each building can be estimated using the U.S. Department of Energy's estimation of



consumption of 16 commercial buildings and three residential models over 16 different climate zones as defined by the U.S. Department of Energy. This algorithm of input data processing from geospatial databases has been obtained from Dr. Pablo Duenas Martinez [9], who originally developed it for the Reference Network Model [18]. The algorithm requires three different types of geospatial data: the building polygon and height information for the estimation of building volume, road lines that lead to the buildings and parcel polygon data that label the land usage (commercial, residential, industrial).



Figure 2-9: Building location with height information

According to the Department of Energy the U.S. is divided into 16 climate zones as shown in figure 2-10: 1A Very Hot Humid, 2A Hot Humid, 2B Hot Dry, 3A Warm Humid, 3B Warm Dry, 3B+ Warm Dry Coast, 3C Warm Marine, 4A Mixed Humid, 4B Mixed Dry, 4C Mixed Marine, 5A Cool Humid, 5B Cool Dry, 6A Cold Humid, 6B Cold Dry, 7 Very Cold, and 8 Subarctic. Each climate zone has 16 commercial building references: Full-Service Restaurant, Hospital, Large Hotel, Large Office, Medium Office, Midrise Apartment, Outpatient Health Care, Primary School, Quick Service Restaurant, Secondary School, Small Hotel, Small Office, Stand-alone Retail, Strip Mall, Supermarket, Warehouse. With the addition of three residential demand profiles for the high, base, and low consumption. The National Renewable Energy Laboratory (NREL) has developed databases on the electricity consumption of the U.S. Department of Energy commercial and residential reference building models of the national building stock as described above.



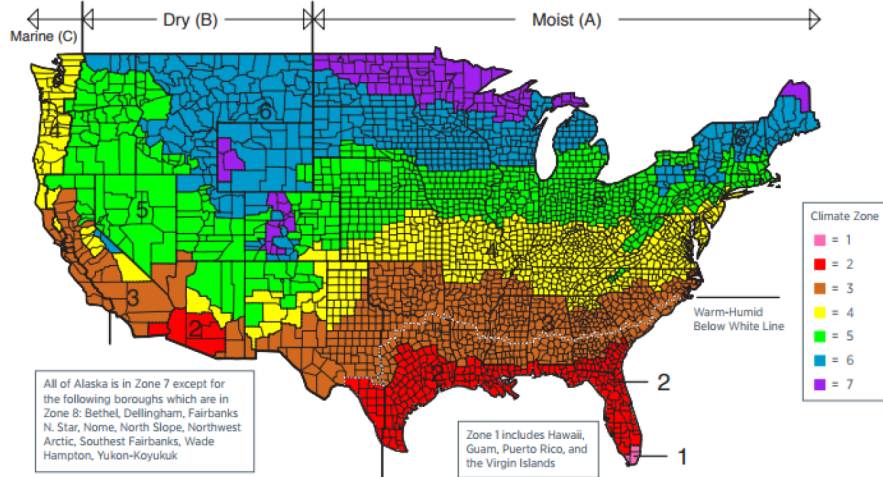


Figure 2-10: U.S. climate regions by county (Department of Energy)

With Puerto Rico being in climate zone 1A Very Hot Humid, the correspondent 19 demand profiles from the U.S. Department of Energy are selected and building reference electricity consumption can be found in the NREL reports [19]. The parcel input data describes the land usage to choose the demand profile correctly, the building data provides the volume of the structure to estimate its consumption better using linear interpolation concerning the reference building models. Adding the electrical substations' locations will enable k-mean clustering of the buildings and therefore assign each building to substation if such data is not known.

This allows for the estimation of electricity demand, peak consumption, and the substation of every identified building. If no such data has been provided about demand, the above method is used for estimation. This algorithm makes it possible to identify the critical infrastructure's demand.

## 2.4 Distribution Network

The input network data used in this research has been gathered from open sources [3], where accuracy and support are not always available. There is no explicit meta-data on how to interpret the primary distribution lines and given their abundance, especially in urban areas as shown in figure 2-11, is time-consuming to sort and label

the distribution network accurately. Therefore, pre-processing of the network input data is needed to be able to standardize it over many executions. A simplification method is proposed below.

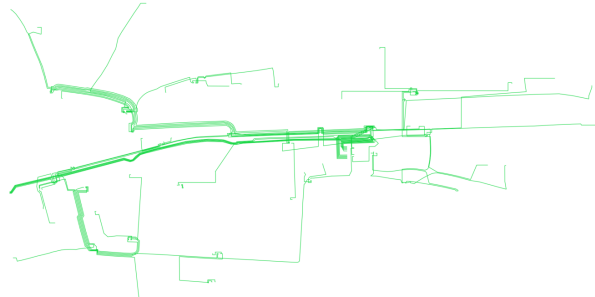


Figure 2-11: Section of primary distribution network in the city of San Juan

### 2.4.1 Simplification

To be able to scale the proposed model developed by this thesis rapidly, the input data must be scalable without significant time consumption. The complexity of the distribution network must be reduced by merging parallel lines into one. This may seem like an oversimplification that may lead to unrealistic results but, keeping in mind that the distribution network is being used to identify the path that must be hardened to connect the critical infrastructure, this will yield acceptable results. The central assumption being made is that any intersection of two lines means that these lines are plugged or there is a switch.

Lines can be aggregated by applying a fixed distance buffer using a geographic information system (GIS) software tools to produce results as in figure 2-12. The buffer represents the right of way for overhead lines or the tunnels for underground lines.

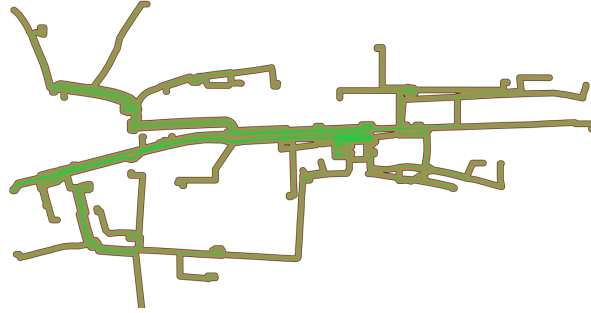


Figure 2-12: Fixed distance buffer of distribution lines in the city of San Juan

## 2.4.2 Polygon to Centerline

Principal channel metrics<sup>2</sup> has been extensively developed both privately and in the open source community [11] mainly for the collection of information for geomorphological research<sup>3</sup>. The buffer created in section 2.4.1 is a bank that can be simplified to get a single line that will serve as the reference to all lines included in the bank.

To get the centerline from the buffer five processing steps have been developed as seen in the workflow figure 2-13: 1) convert buffer polygon to line 2) populate lines with points 3) find the Voronoi polygon of the points 4) extract lines of the Voronoi polygon<sup>4</sup> that are within the initial buffer 5) smoothens the extracted lines to produce centerline.

The more points that populate the lines of the buffer, the higher the accuracy of the results due to the presence of more Voronoi polygons. Since this requires more processing power and run time, a resolution was chosen empirically to maintain the resolution of the network on a macro level since the marginal benefit of finding the exact line length and compute the cost of hardening is below the marginal cost of computation needed to achieve such results.

The result, as seen in figure 2-14, produces many cycles which become very useful in the identification of critical lines in Chapter 3. Two types of lines are defined:

---

<sup>2</sup>Principal channel metrics are methods to identify the centerline of one or multiple given channel (or buffer) shapes, length, local and average width, local and average slope, local and average bank retreat, or the distances from the centerline to the banks respectively.

<sup>3</sup>Geomorphology is the scientific study of the origin and evolution of topographic and bathymetric features created by physical, chemical or biological processes operating at or near the Earth's surface

<sup>4</sup>A Voronoi diagram is a partitioning of a plane into regions based on distance to points in a specific subset of the plane. [4]

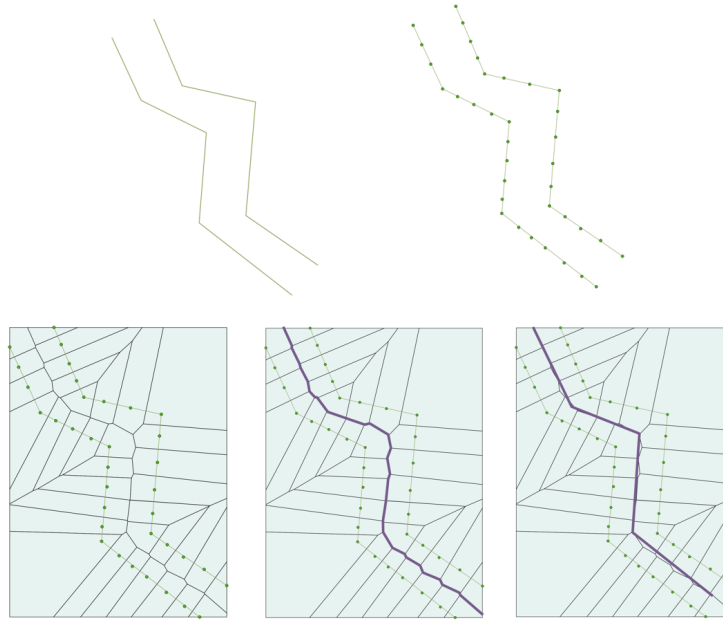


Figure 2-13: Polygon to center line workflow

branches and feeders. Branches connect a node to endpoint (load or substation), and feeders connect nodes. The feeder lines are the centerline of buffers that include multiple distribution lines. The produced meshed structure accounts for the possibility of using or adding switches. This results in a simplified network while maintaining the architecture of the network.

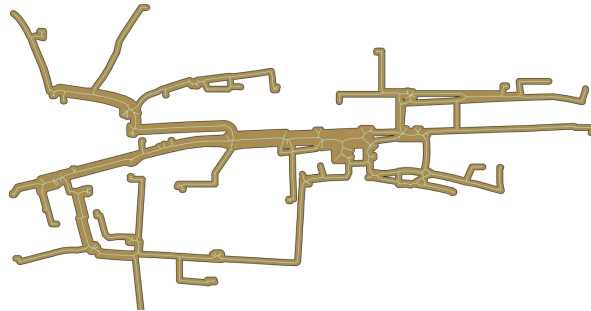


Figure 2-14: Center line of buffer

# Chapter 3

## Critical Infrastructure

### 3.1 Critical Demand

Even though a hurricane can cause devastation on the island, the number of direct deaths was much lower than the number of indirect deaths for the case of Puerto Rico. This is mainly due to disabled services such as hospitals and sanitation facilities. Unmanageable chaos increases crimes of desperation and lack of options. Hence the need for prompt service post-natural disaster to maintain the critical level of life. The essential needs of a human being are physiological and safety: physiological needs include shelter and water, safety needs include health. Based on these needs a list of critical facilities is identified [20]:

- Hospitals and health care centers
- Sanitation facilities
- Water treatment facilities
- Government offices
- Shelters and Hotels
- Schools and universities
- Ports and Piers

Hospitals and health care centers provide emergency services and disaster relief if such facilities do not have power their usability drops and crime rate increases. Sanitation facilities ensure access to clean water, which in the case of Puerto Rico was a significant problem. Government offices must stay operational to maintain order and the rule of law even under stressful conditions. Many homes will be damaged and destroyed due to the natural disaster; people will be designated to shelters and sometimes hotels until restoration takes place. Loss of power for almost a year can significantly deteriorate the quality of education, and therefore, educational institutions must maintain operation to ensure a continuation of the way of life.

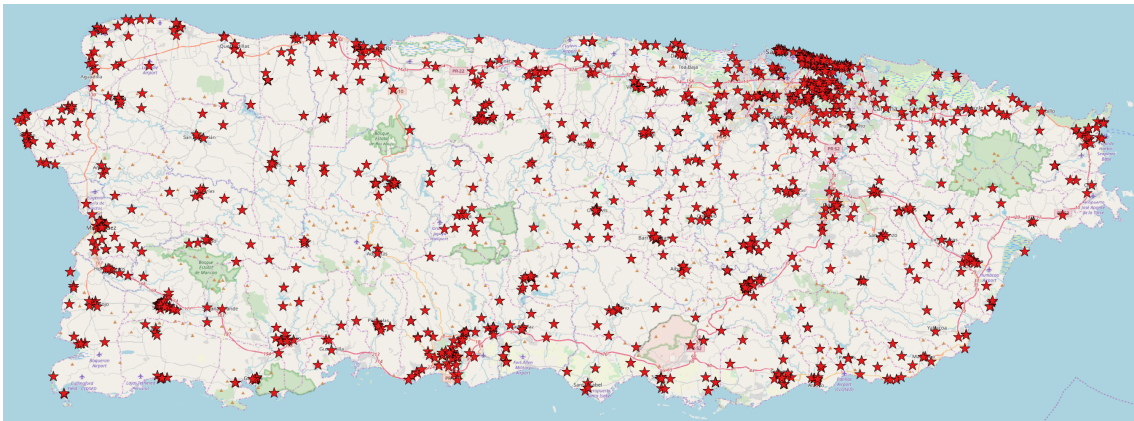


Figure 3-1: Location of critical infrastructure in Puerto Rico

For ease of optimization, the above facilities are labeled under one of three demand profile types: residential, commercial, and infrastructure. Residential includes shelters and hotels, commercial includes offices and educational institutions, and infrastructure includes hospitals, facilities, and ports.

### 3.1.1 Load Profiles

The U.S. Department of Energy provides demand profiles for different locations in the mainland United States, which are good indicators of demand patterns throughout the day and year [2]. Given how climate has a significant impact on electricity demand, choosing a location close to Puerto Rico is an educated guess of what the demand profiles would look like on the island. Key West, Florida, will serve as the benchmark

for the demand estimation.

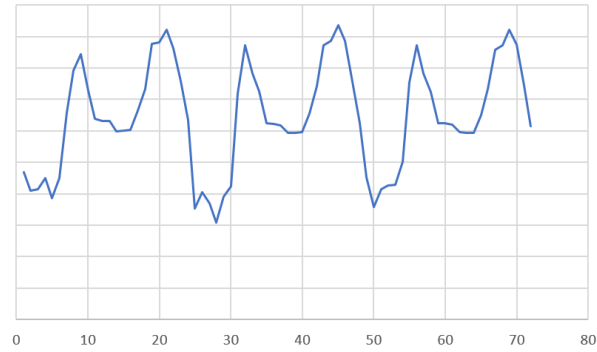


Figure 3-2: Normalized 3 day residential demand profile from Key West, FL

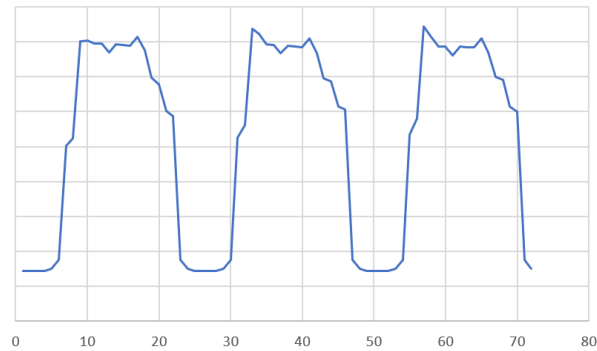


Figure 3-3: Normalized 3 day commercial demand profile from Key West, FL

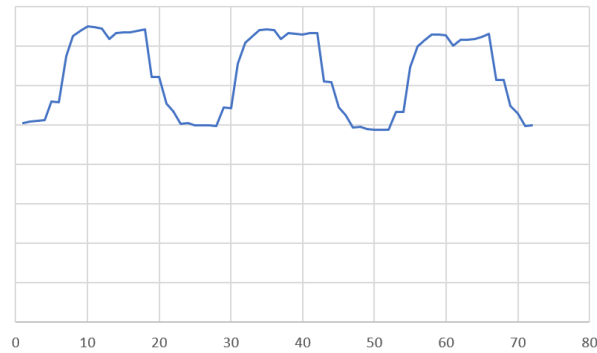


Figure 3-4: Normalized 3 day infrastructure demand profile from Key West, FL

## 3.2 Critical Lines

The principal channeling algorithm developed in chapter 2 simplifies dense electrical network layout to a single line architecture. Figure 3-5 shows that the macro level architecture of the network has been preserved and the network is much faster to process.

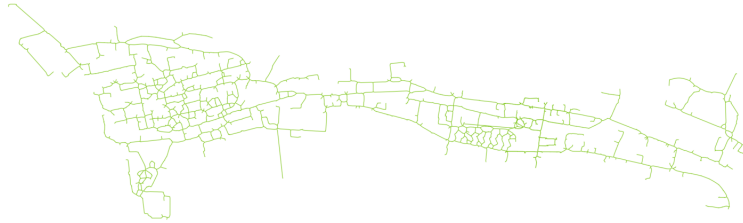


Figure 3-5: Simplified primary distribution network of the city of San Juan

The goal of this section is to identify the primary distribution lines that are critical to the defined loads. Binning the loads to their correspondent MV/LV substation allows the identification of the territory of interest, which are all the lines that reach or connect to the critical loads and their substation.



Figure 3-6: Downtown San Juan: Critical Loads (Stars), Substation (Triangle)

### 3.2.1 Steiner Tree

Once the territory is identified as in figure 3-6, two combinatorial optimization problems need to be applied to find the critical lines that connect the critical loads: non-negative shortest path and minimum spanning tree. This procedure is also known



under the umbrella term of Steiner tree [22]: in a graph (distribution network) with non-directed non-negative weighted edges and defined subset of vertices called terminals (critical loads), the Steiner tree is a graph of minimum weight that must contain all terminals and may contain additional vertices. If the terminals subset includes only two vertices, then the Steiner tree is a weighted shortest path problem, and if the terminals subset includes all the vertices, then the Steiner tree is the minimum spanning tree of the graph.

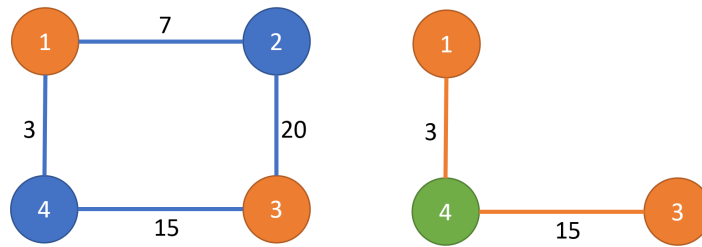


Figure 3-7: Simple Steiner Tree Example <sup>1</sup>

Even though both the minimum spanning tree and shortest path problems are solvable in polynomial time, the Steiner tree is an NP-complete<sup>2</sup> decision problem or NP-Hard. This implies that the problem does not scale well when the number of edges in the network increases. Moreover, the problem takes longer to solve when the initial graph is more meshed since there will be multiple paths to connect terminals.

### 3.2.2 Triangulation

Network cycles heavily exist in the simplified distribution network produced in chapter 2, particularly in urban areas. It is then imperative to speed up the Steiner tree problem so that it converges to an approximation of a solution in an acceptable time. The most obvious way to speed up the algorithm is the simplification of the network.

<sup>1</sup>Blue nodes are vertices of the original weighted graph on the left, orange nodes are the identified terminals, the Steiner tree solution on the right connects the terminal nodes via shortest path and minimum spanning tree, the green node is a Steiner vertex.

<sup>2</sup>NP: non-deterministic polynomial-time

Two types of nodes are identified: intersection nodes and end nodes; intermediate nodes are generally not considered unless they are terminal nodes.

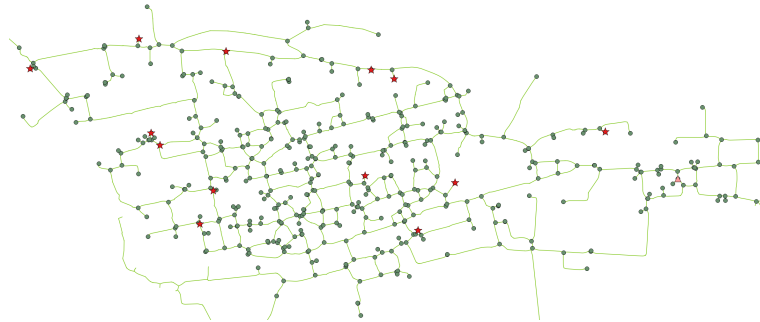


Figure 3-8: Network nodes of Downtown San Juan

The Delaunay triangulation<sup>3</sup> is the dual graph of the Voronoi diagram which partitions planes into regions based on distance. The Delaunay triangulation is created from the intersection of circles whose centers are the extremities of the Voronoi diagram cells. When setting the edges of the Delaunay triangulation the algorithm  $DT(P)$  maximizes the smallest angle of the triangles in the triangulation, in other words, it attempts to minimize acute angles. In certain instances this might not be the best solution, as highlighted in red in figure 3-9 the existing connection of two nodes is dominated by many triangulation edges which result in a longer than necessary connection. Therefore, modification to the Delaunay triangulation is required to take into account the existing network layout.

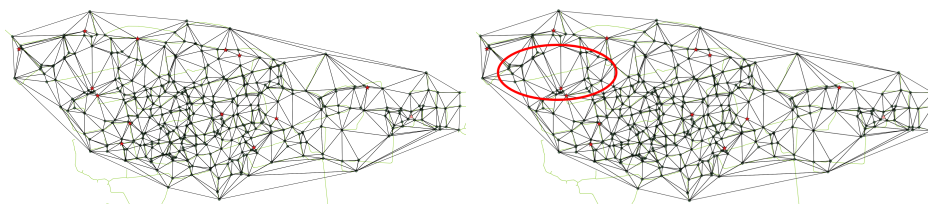


Figure 3-9: Delaunay triangulation of nodes

Starting with the Delaunay triangulation, removing edges from the triangulation that intersect with edges in the existing network as seen in 3-9, the original network layout is preserved. Removing triangulation edges whose network edges include more

---

<sup>3</sup>Delaunay triangulations maximize the minimum angle of all the angles of the triangles in the triangulation; they tend to avoid sliver triangles.

than the starting and ending nodes reduces redundancy of paths. Including any edges that are not yet considered results in a modified Delaunay triangulation that is suitable for the Steiner tree problem.



Figure 3-10: Triangulation results for Downtown San Juan

The produced tree is a trimmed down version of the Delaunay triangulation that includes the simplified graph edges only. The primary purpose of this triangulation is the omittance of redundant edges between two nodes by considering the weight of the shortest edge only and ignoring long connections that will not be useful for the Steiner tree algorithm.

### 3.2.3 Algorithm

Extensive research has been devoted to better approximate Steiner trees in larger and more complex network [12]. The derived algorithm below produces a tree solution whose weight is within  $2 - (2/t)$  factor of the weight of the optimal solution<sup>4</sup>, where  $t$  is the number of terminal nodes. This minimizes the number of branches by searching for a single path that includes as many terminals as possible.

A complete graph where the edges are weighted by the shortest path distance between the nodes has already been produced in the triangulation. Taking the subgraph of terminal nodes and finding its minimum spanning tree will result in an approximate solution in an acceptable time frame. From the Steiner tree algorithm resulting path, the critical lines in the primary distribution network can be easily identified, as shown in figures 3-11 and 3-12.

---

<sup>4</sup>The weight of a tree edge is defined by the distance of the line it represents



Figure 3-11: Intermediate results: critical path of Downtown San Juan

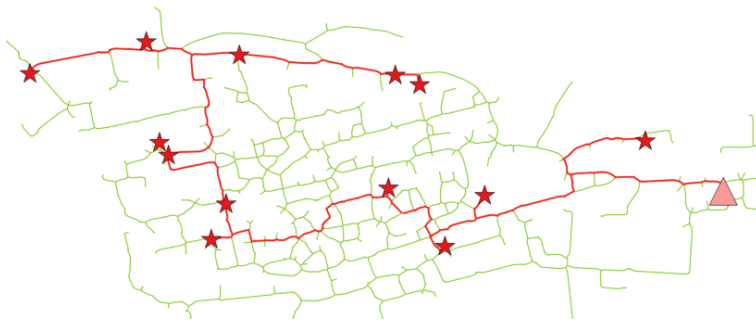


Figure 3-12: Final results: critical lines of Downtown San Juan

# Chapter 4

## Microgrid Design

### 4.1 Overview of Microgrid Design

Natural disasters can cause extreme damage to the electrical grid and therefore, prevent the transmission of power from generation facilities to consumers, particularly critical infrastructure. To avoid this problem, distributed generation and storage resources can be placed at the MV/LV substation of the critical networks identified in chapter 3. Redundancy of generation is required to ensure an acceptable level of reliability given the extraordinary circumstances introduced in chapter 1. Designing an island solution becomes necessary to ensure availability of power regardless of the status of the main grid.

It is assumed that the main grid is the more economical option, and under normal conditions, the off-grid solution is not used. Hence, the deployment of the distributed energy resources may be set up and operated as microgrids [23]. Micro or mini-grids are clusters of electricity loads and sources that are typically connected to the main grid but can also disconnect and operate autonomously to become islanded under particular conditions.

The generation required to meet the demand of the clustered critical infrastructure from chapter 3 can be sized using the linear programming model described in this chapter. The main objective of the model is to determine the minimum present cost combination of diesel generators, photovoltaics and battery storage units over the

meaningful life of the project given the different demand profiles from section 3.1.1, technical and financial constraints. Energy dispatch resulting from the optimization provides an educated estimate of the leveled cost of energy demanded. The linear programming model also provides a view of the total investment needed to build the microgrid system as well as what type and size of technologies to install given demand and parameter variations.

## 4.2 Microgrid Components

Under extraordinary natural conditions, distributed energy resources can be easily protected due to their smaller size and thus become more attractive to policymakers in the Puerto Rican government. The consistently decreasing cost of solar panels, as well as their stack-able shape, become the focal point of designing microgrids. Battery storage is charged when there is an excess of solar energy, or the diesel generator is operating. When both solar and battery cannot meet the demand, diesel generators are deployed.

Solar radiation data is available on an hourly basis in  $W/m^2$ . Given that a typical solar panel has an area of  $1.6m^2$ , the available solar energy in Watts on an hourly basis for 8760 hours accompanies the demand profiles from section 3.1.1 as inputs to the optimization model.

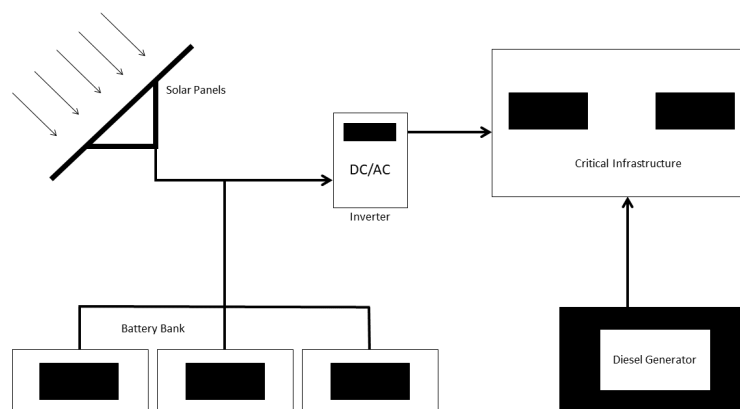


Figure 4-1: Microgrid Topology

### 4.2.1 Solar Panels and Battery Storage

The main constraints relating to photovoltaics are the radiation of the sun and the available space to place the panels. Urban areas are more structurally and demographically dense than rural areas, and this must be taken into consideration when evaluating critical infrastructure. Demographic density increases the energy demand and the critical infrastructure, while structural density limits the available space of installing solar panels. In rural areas, there is abundant space to install solar panels. By this logic, two different types of projects are identified: rural and urban. Where the maximum number of solar panels that may be installed is smaller in urban areas than the rural ones. This constraint is essential because, for a case such as Puerto Rico, where sunlight radiation is abundant in the day, results show that this constraint is often the hard limit of the nominal capacity of solar energy.

### 4.2.2 Diesel Generator

As shown in table A.1 in Appendix A, the investment cost in USD per kilo-Watt decreases as the rated capacity of the installed generator increases. Economies of scale in generator options must be taken into consideration when optimizing and therefore the model is programmed to choose one of the generators from the list<sup>1</sup> with its respective rated capacity and investment cost using binary values [16]. This introduces integer values to the optimization since the nominal capacity of the diesel generator installed is constrained by its rated capacity and investment cost.

Diesel generators require fuel tank storage to be sized for an interval of time depending on the frequency of fuel shipments to the territory. These tanks are sized by running the optimization model with the base fuel cost<sup>2</sup> only. This allows for the sizing of the fuel tank that meets the demand for a given interval of time. The lowest cost of fuel will produce the largest fuel tank, and therefore it is adopted as such.

---

<sup>1</sup>The Rural Electrification Model developed by MIT/Comillas research group has a library of diesel generators which were used here.

<sup>2</sup>Excluding overhead cost of transportation.

## 4.3 Critical Operation

### 4.3.1 Transportation Cost

The purpose of designing the critical microgrids is to ensure the continuity of electricity supply to the critical infrastructure under extraordinary circumstances such as hurricanes and natural disasters. Looking particularly at what has transpired in Puerto Rico, hurricane Maria not only caused damage to the electrical grid but also to roads which made mobility highly difficult, especially reaching rural villages. As previously discussed, diesel generators require fuel tanks which themselves require periodic delivery of fuel. Given the same classification of territories: urban and rural, transportation cost and delivery time must be accounted for.

Postnatural disaster, immediate operation of the critical infrastructure is required. Solar panels and batteries do not require extensive external maintenance since photovoltaic cells convert photons of light to electrical energy and storage batteries are for converting electrical energy to chemical energy and vice versa. When it comes to diesel generators; there is a dependence on fuel availability, which is dictated by transportation. After a natural disaster, road damages can disable travel and therefore hinder transportation abilities. The implications are stronger in areas further away from energy supply hubs (ports).

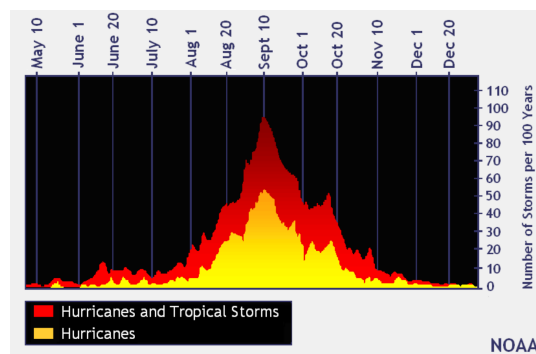


Figure 4-2: Hurricane Season

To account for these externalities and looking at the NOAA's hurricane and tropical storm data for the US shown in figure 4-2, a transportation fee, and penalty during hurricane season (August to October) must be added to the base cost of the



fuel.

After running the model the first time with the base fuel cost only, the variable **fu** (presented in section 4.4.2) indicates the liter amount of diesel consumed in a single period for each hour of the year. These amounts are aggregated and summed in intervals of three weeks, which reflects a supposed delivery schedule of fuel shipment needed to fill the tanks of the diesel generators at base cost. This results in a profile of the fuel required every three weeks, the transportation cost for any given interval of three weeks can be extracted from tables A.3 and A.4 in Appendix A for rural and urban territories respectively. Transportation cost increases when the amount of fuel that needs to be delivered increases. Thus, a linear relationship is proposed based on the assumption that more fuel requires more equally sized delivery trucks.

A fuel cost profile is constructed by adding the transportation cost of every period (one hour) to the base cost of fuel, periods from the same interval will have the same transportation cost since the total delivery cost can be divided equally on each liter of fuel. Periods from different intervals will have different transportation cost depending on the total amount of fuel in the tank required at a base cost to meet the demand of the system.

To emphasize the difficulty of delivering fuel post natural disasters, a penalty of 10 cents is applied to the fuel cost in the interval of time during hurricane season. Using this penalty, along with the transportation cost, will make diesel generation a less favorable choice due to the compounded high cost of fuel associated with it.

### 4.3.2 Demand Mix

Each microgrid system has a different mix of demand types from section 3.1.1 that must be accounted for when optimizing. Thus a hybrid profile is composed based on the weighted sum of the standard demand profiles.

The three demand profiles identified are residential, commercial, and infrastructure. Each microgrid system will have a mixture of these three profiles if not a single one. Taking these standard demand profiles and normalizing them generates per-unit profiles for each hour. Multiplying the demand type percentage of the total demand

by the normalized profile produces a normalized weighted sum.

$$D = A \sum_{s=1}^3 w_s d_s \quad (4.1)$$

Multiplying the sum by the peak demand generates demand profile  $D$  that reflects the weighted average hourly demand profile of total demand.

## 4.4 Modeling Components

The parameter components are the input data being considered by the model. The variables are the components that will hold the output data once the optimization is completed. Given the objective function and constraints, a linear programming optimization model is built as detailed in the following subsections.

### 4.4.1 Parameters

#### System

- s** Scenario demand profile
- T** Period in hours: 8760
- t** Single period: 1
- i** Generator Size from table A.1
- w** Scenario weight
- D** Energy demand
- voll** Value of lost load in Watts: 0.001
- tol** Lost load tolerance: 0%
- n** Project life in years: 20
- $\Delta_t$  Time period in hours: 1
- da** Debt-to-Asset Ratio: 0 %
- r** Interest Rate: 6 %
- d** Discount Rate: 12%

## Solar

<b>pvc</b>	Single solar panel nominal capacity in Watts: 300
<b>pveff</b>	Inverter efficiency: 98 %
<b>sol</b>	Available solar radiation for the period
<b>pvom</b>	Operation and maintenance cost in USD perWatts: 0.005
<b>pvi</b>	Investment cost in USD per Watts: 0.5
<b>maxu</b>	Maximum amount of solar panels that can be installed in rural territory: 1000
<b>maxu</b>	Maximum amount of solar panels that can be installed in urban territory: 300

## Battery

<b>cheff</b>	Charging efficiency: 95 %
<b>diseff</b>	Discharging efficiency: 95%
<b>mct</b>	Maximum charging time in hours: 5
<b>mdt</b>	Maximum discharging time in hours: 5
<b>dod</b>	Depth of discharge: 20 %
<b>batom</b>	Operation and maintenance cost in USD per Watts: 0.005
<b>bati</b>	Investment cost in USD per Watts: 0.5

## Diesel Generator

<b>geneff</b>	Generator efficiency: 30 %
<b>lhv</b>	Low Heating Value in Watts per Liter: 9890
<b>fc</b>	Diesel base cost in USD per Liter: 1.0
<b>ftc</b>	Diesel transportation cost in USD per Liter: 1.0
<b>genom</b>	Operation and maintenance cost in USD per Watts: 0.01
<b>genic</b>	Generator investment cost A.1
<b>gens</b>	Generator size in kiloWatts A.1

## 4.4.2 Variables

### System

<b>npc</b>	Present cost
<b>omc</b>	Total operation and maintenance cost
<b>ic</b>	Total investment cost
<b>ll</b>	Amount of lost load in Watts
<b>llc</b>	Cost of lost load in USD
<b>curt</b>	Energy curtailment in Watts

### Solar

<b>pvw</b>	Total solar energy output in Watts
<b>pvu</b>	Total number of installed solar panels

### Battery

<b>batc</b>	Maximum capacity in Watts
<b>fin</b>	Energy inflow in Watts
<b>fout</b>	Energy outflow in Watts
<b>soc</b>	State of charge in Wh
<b>mcp</b>	Maximum charging power in Watts
<b>mdp</b>	Maximum discharging power in Watts

### Diesel Generator

<b>geni</b>	Generator investment cost in USD
<b>genc</b>	Maximum capacity in Watts
<b>fu</b>	Diesel consumed
<b>genw</b>	Total diesel generator energy output in Watts
<b>fuc</b>	Generator variable cost
<b>gen</b>	Generator option (binary)

### 4.4.3 Objective Function

The objective function minimizes the present cost of each scenario multiplied by the weight of the scenario. The present cost is constituted of the investment cost, operations and maintenance cost, fuel cost, and lost load cost.

$$npc = \sum_s (ic + omc + fuc + llc) * w_s \quad (4.2)$$

### 4.4.4 Constraints

#### Energy

Demand balance equation:

$$D_{s,t} = pvw_{s,t} + genw_{s,t} + fin_{s,t} - fout_{s,t} + ll_{s,t} - curt_{s,t} \quad (4.3)$$

Maximum amount of non-served energy allowed by the system given the tolerance parameter:

$$tol \geq \frac{\sum ll_{s,t}}{\sum D_{s,t}} \quad (4.4)$$

#### System

Operations and maintenance cost of the system:

$$omc = (genc * genom + batc * batom + pvu * pvc * pvom) * \frac{1}{(1+d)^n} \quad (4.5)$$

Initial investment cost of the system:

$$ic = geni + (batc * bati) + (pvu * pvi * pvc) \quad (4.6)$$

Total fuel cost including transportation cost profile:

$$fuc_s = \sum \frac{fu_{s,t} * fc_t}{(1+d)^n} \quad (4.7)$$

Cost of non-served energy:

$$llc = \sum \frac{\sum ll_{s,t} * voll}{(1 + d)^n} \quad (4.8)$$

## Solar

Output of solar energy is limited by the radiation of the sun and the number of installed solar panels:

$$pvw_{s,t} \leq sol_{s,t} * pveff * pvu \quad (4.9)$$

$$pvw_{s,t} \leq pvc * pvu * \Delta_t \quad (4.10)$$

Number of solar panels that may be installed is limited by the available space in the territory of the system:

$$pvu \leq maxu \quad (4.11)$$

## Battery

Charging and discharging power of the battery:

$$mcp = \frac{batc}{mct} \quad (4.12)$$

$$mdp = \frac{batc}{mdt} \quad (4.13)$$

Energy flow of the battery:

$$fin_{s,t} \leq mcp * \Delta_t \quad (4.14)$$

$$fout_{s,t} \leq mdp * \Delta_t \quad (4.15)$$

State of charge of the battery, initially the battery is assumed fully charged:

$$soc_{s,0} = batc + fin_{s,t} * cheff - \frac{fout_{s,t}}{diseff} \quad (4.16)$$

$$soc_{s,t} = soc_{s,t-1} + fin_{s,t} * cheff - \frac{fout_{s,t}}{diseff} \quad (4.17)$$

Minimum depth of discharge and maximum charge of the battery:

$$soc_{s,t} \leq batc \quad (4.18)$$

$$soc_{s,t} \geq batc * dod \quad (4.19)$$

## Diesel Generator

Generator nominal capacity from library of generators in table A.1:

$$genc \leq \sum_i gens_i * gen_i \quad (4.20)$$

Generator choice from library of generators in table A.1:

$$\sum_i gen_i = 1 \quad (4.21)$$

Generator output given generator nominal capacity:

$$genw_{s,t} \leq genc * \Delta_t \quad (4.22)$$

Amount of diesel consumed given the generator of choice's output and parameters:

$$fu_{s,t} = \frac{genw_{s,t}}{geneff * lhv} \quad (4.23)$$

Generator investment cost from library of generators in table A.1:

$$geni = \sum_i genic * gen_i \quad (4.24)$$

## 4.5 Results

While the accuracy of the produced results is not to be compared with the Local Rural Electrification Model, the usage of continuous variables and simplification of constraints can produce indicative preliminary results that serve well for reliability planning which is the core of the problem.

### 4.5.1 Case Results

Two cases of the state of San Juan with solar radiation data from 2018 are presented. Presenting both urban and rural scenarios highlights the difference in results from one territory to another. The critical demand of the territory is set to 50 kW with equal weights  $w_s$  for the load profiles.

#### Urban

The Net Present Cost of the microgrid is 296 Thousand USD with a Levelized Cost of Electricity of 0.14 USD/kWh. The initial investment required is 181 Thousand USD with a yearly operations and maintenance cost of 22 Thousand USD. The maximum amount of solar panels were installed with battery capacity of 450 kW and a 20 kW generator.

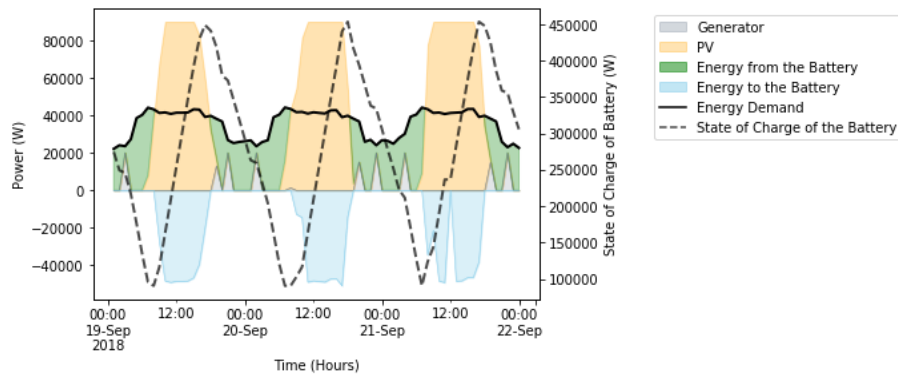


Figure 4-3: Urban San Juan: energy dispatch for 50 kW microgrid



## Rural

The Net Present Cost of the microgrid is 255 Thousand USD with a Levelized Cost of Electricity of 0.12 USD/kWh. The initial investment required is 205 Thousand USD with a yearly operations and maintenance cost of 24 Thousand USD. 511 solar panels were installed with battery capacity of 460 kW and a 20 kW generator.

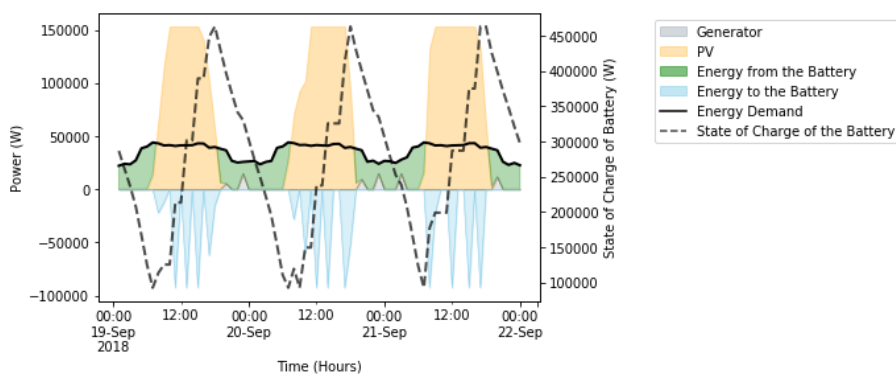


Figure 4-4: Rural San Juan: energy dispatch for 50 kW microgrid

### 4.5.2 Library of Microgrids

Discretizing the weights of the different demand profiles into  $w_s = [0, 0.33, 0.66, 1]$  yields ten combinations of normalized demand profiles with different magnitudes  $A$  representing the demand of the microgrid in kW. Running all 10 cases for various energy demands results in 10 levelized costs of energy per demand type. Aggregating these results produces a 5D Average cost curve (1 dimension for each demand profile, one dimension for peak demand, one dimension for cost) that we can linearly interpolate from rather than optimize at every instance.

However, the linear program developed in this chapter is not significantly time-consuming: a single run takes 180 seconds. Given no time constraints to execute code this optimization problem can be formulated into a single function that can be called with all relevant inputs to deliver the essential outputs needed for segmentation and clustering of different microgrids. For the sake of simplicity, this method has been chosen, and the average cost curve is not developed further.

THIS PAGE INTENTIONALLY LEFT BLANK

# Chapter 5

## Network Reliability

### 5.1 Overview of Reliability

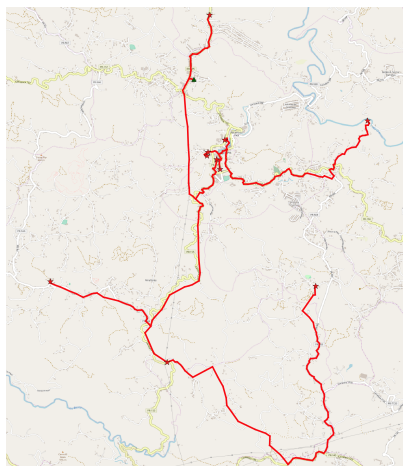
After processing the input data, identifying the critical infrastructure and sizing of microgrids, the results so far are at the MV/LV substation level. However, the layout of LV lines obtained in Chapter 3 has to be reconsidered now, as it may not be compliant with some reliability requirements that we may want to prescribe. Specific critical loads are located far away from the substation, thus requiring a single long line to reach it. Such lines will have high failure rates and must be looked at carefully. Moreover, cost savings can be achieved by clustering together substations and connecting them through the MV network. As noted in Chapter 4, some economies of scale exist in microgrid generation cost. Taking advantage of already existing underground lines in urban areas and economies of scales will serve as the cost minimization terms for the resiliency of the network. A minimal network infrastructure, as identified in Chapter 3, can rarely be considered reliable, especially when the critical load is significantly far away from the substation where the generation is located. Therefore, reliability constraints must be applied, given cost minimization, to produce an acceptable and reliable network.

## 5.2 Distance Metrics

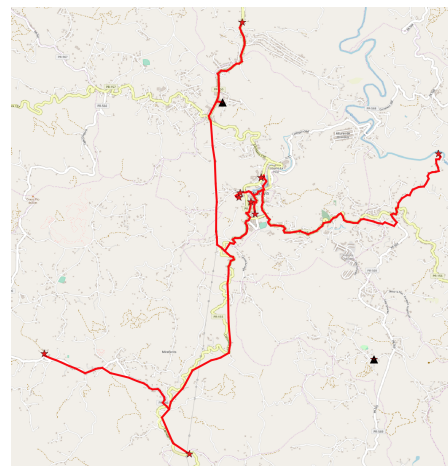
### 5.2.1 Segmentation

Segmentation is defined as the removal or reinforcement, of unreliable low voltage lines that are identified as individually unreliable due to their length from the connection point to the critical load.

Looking initially at every extremity load node, if the branch that connects the load node to its parent node (i.e. intermediate load node or Steiner vertex) is below the acceptable reliability threshold then this branch must be eliminated from the critical network and the load node becomes a stand-alone system <sup>1</sup>. Such a decision is driven by the following thought process: if an individual branch line is below the acceptable reliability threshold then that line is too long. Even if the network upstream has maximum achievable reliability, the reliability of the load node from that branch will drop to below the threshold. Since that line is too expensive and reinforcing it with addition of a new line will have a great cost to benefit ratio, the best option is to break that load away from the network and install generation that meets its individual demand.



(a) Steiner tree



(b) Segmented Steiner tree

Figure 5-1: Critical infrastructure for the village of Orocovis

Such cases mainly arise in rural areas where specific critical loads are spread out.

---

<sup>1</sup>A stand-alone system is defined by the placement of generation at the location of demand

Given the high cost of undergrounding and the sparsity of the network, the cost of hardening an individual long line that reaches a single critical load is rarely justifiable. Therefore, this model rejects such hardening and will always opt into a stand-alone system. Also, if the territory served by an MV/LV substation includes only one critical load, the load is also converted into a stand-alone system since the need of reinforcing lines is not necessary because a network by definition does not exist. Such conversion assumes that the critical load is far from another substation, hence the exploration of connecting to a different substation is not developed in this research.

This segmentation of the critical network reduces it to a core with acceptable length lines that may be used to better cluster microgrids together. Up to this point, the process does not deal with unreliable primary and secondary trunks as defined in section 5.3, this will be further discussed in section 5.4.

### 5.2.2 Clustering

Clustering is defined as the grouping of microgrids through the medium voltage network, that connects MV/LV substations, to aggregate generation in one place while taking advantage of the existing underground infrastructure and economies of scale in generation options.

After segmentation and the elimination of long unreliable lines, the critical loads are served by either microgrid generation through the existing network substation or as a stand-alone generation placed at the location of the critical load. The stand-alone systems are considered final results since they have been labeled too expensive to harden and their extension lines unreliable due to length. Then, the clustering process only considers the loads that remain connected to the MV/LV substation. The main purpose behind the centering of microgrid territories around existing MV/LV substations is the ability to cluster them while taking advantage of the existing infrastructure at MV Level. The generation of the cluster is then placed at the weighted center of the substations.

After properly sizing the demand being served by the MV/LV substations and the identification of the MV lines that interconnect them, the MV network is considered

to be radial. Thus, a tree of substation nodes is the initial state, as shown in figure 5-2. Meshed networks and lines that create loops in the MV networks are not considered in this phase since the purpose is to find the minimum cost of clustering microgrids. Reliability measures are applied in the following section.

The algorithm starts with the initial state of full network connecting where all the substations being evaluated are connected via MV lines. Each cluster is defined by:

- Total demand which is equal to the sum of demand of microgrids in the cluster
- Total generation cost computed in using Chapter 4
- Total cost of hardening all the MV lines in the cluster

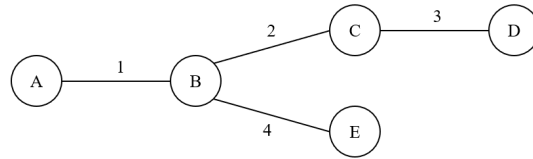


Figure 5-2: Clustering Example: Case 1

Figure 5-2 illustrates an example of numbered MV lines and labeled substation nodes. Given N nodes, N-1 lines will be evaluated. Case 1 cluster is identified by:

- Total demand:  $D_{Case1} = \sum D_n = D_A + D_B + D_C + D_D + D_E$
- Generation cost:  $GenCost_{Case1} = GenCost(D_{Case1})$
- Line hardening cost:  $HD_{Case1} = HD_1 + HD_2 + HD_3 + HD_4$

There is a need to identify the line that divides the network into the two largest possible clusters based on the demand weight of each substation node. For the sake of simplicity, the clustering example nodes will have equal weights. One approach to identifying the line of interest is looking at the weight of the nodes it joins from either side. Line 2 connects A, B and E on one side and C and D on the other side, making it the line that connects the two largest subgroups. This process can be generalized

over the vast radial network through a drop down approach of all the lines in the network with acceptable run time. Processing time can be increased by selecting from primary trunk lines <sup>2</sup> first since they are the intermediate lines in the network.

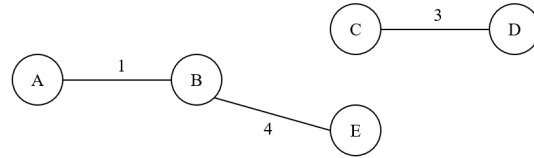


Figure 5-3: Clustering Example: Case 2

Removing line 2 results in two smaller clusters (A, B, E) and (C, D) which will be identified as Case 2.1 and Case 2.2 respectively. Case 2 clusters are identified by:

- Total demand:  $D_{Case2.1} = D_A + D_B + D_E$
- Total demand:  $D_{Case2.2} = D_C + D_D$
- Generation cost:  $GenCost_{Case2.1} = GenCost(D_{Case2.1})$
- Generation cost:  $GenCost_{Case2.2} = GenCost(D_{Case2.2})$
- Line hardening cost:  $HD_{Case2.1} = HD_1 + HD_4$
- Line hardening cost:  $HD_{Case2.2} = HD_3$

To evaluate which state to adopt a simple cost analysis is carried out. If the sum of costs (generation + hardening) in Case 1 is lower or equal to the sum of costs of both clusters of Case 2. If Case 2 is the better option, the present state becomes Case 2, and the process is repeated over the two new clusters. The algorithm exists when the new state is equal to the initial state: if Case 1 is a better option than Case 2, no changes occurred, therefore, the algorithm exists.

This clustering algorithm finds the answer to the question: Are economies of scale in generation saving enough to justify the MV line hardening cost?

---

<sup>2</sup>Lines types are explained in section 5.3.1

## Hardening Cost

This USD per kilometer value is an input to the system. The higher the value is the less clusters the algorithm will produce: a value of 0 will produce a single cluster of all the substations being studied. A value of 0 is inputted when considering existing underground MV lines since underground cables are considered hardened.



Figure 5-4: Isleta de San Juan cluster of microgrids

Figure 5-4 shows the results of the clustering algorithm in the Isleta de San Juan, which includes three substations. The red stars are the critical loads, and the red lines are the Steiner critical lines, the green triangles are the MV/LV substations, the black triangle is the generation sight of the cluster, the blue lines are the MV lines.



Figure 5-5: Electric System Islands Identified. Source: PREPA Recovery and System Resiliency Roadmap



In the case of Puerto Rico studied throughout this thesis, the initial clusters are adopted from the island systems identified by PREPA [5]. Figure 5-5 highlights the territories which PREPA has designated to become microgrid territories for an emergency operation.

## 5.3 Failure Rate

### 5.3.1 Line Types

Two types of distribution lines are identified in the Steiner tree: the main trunk and branches. The primary trunk connects the substation to the Steiner vertices, and the branches are the edges that go from Steiner vertices to load nodes. In larger networks, secondary trunks may exist where they connect Steiner vertices to a Steiner vertex on the main trunk or to an intermediate load node. In figure 5-6 as seen below the substation is a yellow triangle, the loads are blue nodes, the Steiner vertices are orange nodes, the primary trunk is an orange line, the secondary trunks are green edges, and the branches are gray edges.

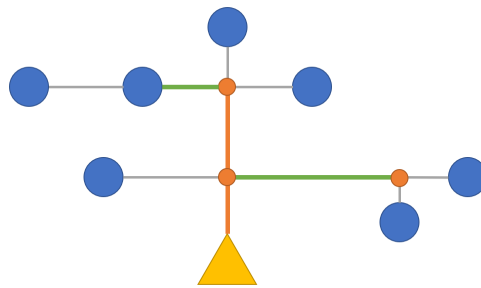


Figure 5-6: Sample Graph

It is essential to note the difference between these lines because their failure rates will differ and will impact the results of the reliability algorithm. It is also evident that reducing the rate of failure of the main trunk will have the most impact since the individual edges of the main trunk are collectively exhaustive of the load nodes in the network [7].

### 5.3.2 Equipment Failure

System reliability models have been developed to use average equipment failure rates that are laboratory tested with the equipment. These rates are seldom indicative of the real failure rate of electrical equipment under various conditions, not to mention hurricanes and storms. Failure rate modeling customization using inspection data has been developed in [cite Brown] using a condition score based on a set of criteria such as age and loading history. This is an interpolation method based on a normalized condition score that reflects the assumption about the equipment. The condition score is calculated through the following equation:

$$ConditionScore = \frac{\sum_{i=1}^n w_i r_i}{\sum_{i=1}^n w_i} \quad (5.1)$$

Where  $r_i$  and  $w_i$  are the normalized score and weight of the criterion respectively.  $r_i = 0$  represents the best inspection results,  $r_i = 1$  represents the worst inspection results. The failure rate is then calculated using the following equation:

$$\lambda(x) = Ae^{Bx} + C \quad (5.2)$$

Where  $\lambda$  is the failure rate,  $x$  is the condition score and A, B, C are condition parameters derived through benchmarking. This equation has been empirically developed [6] and yields the following results for underground equipment.

Equipment	$\lambda(0)$	$\lambda(1)$
MV Line	0.015	0.025
Primary Cable	0.00186	0.368
Secondary Cable	0.00311	0.0932
Substation Transformer	0.0075	0.14
Transformer	0.0005	0.1
Switch	0.0005	0.01
Splices and Joints	3E-5	0.318

Table 5.1: Failure rate of underground equipment (per year value)

Cables and lines<sup>3</sup> failure rate are failure rates per circuit kilometer. A linear relationship with slope  $\lambda$  has been adopted since the failure rate is small enough that a non-linear relationship at the distribution level is not necessary. Moreover, as highlighted in [13] the rate of failure relationship with the short distance MV lines is approximately linear.

Normalizing the per year value over 365 days will yield the normalized failure rate of the equipment, its one's complement is interpreted as the reliability of the equipment. The data in table 5.1 has been collected from U.S. equipment under normal operations. Such data is not representative of failure rates of equipment under hurricane conditions and discusses damages utilities have suffered from past hurricanes in North America [7]. Data collection on equipment failure under normal conditions let alone hurricanes is minimal and to certain utilities not encouraged due to exposure purposes beyond the scope of this research. Therefore, the input of the rate of failure of the various equipment in the electric distribution network becomes a policy topic whose results are related to the hardening investment cost needed to maintain an acceptable level of service.

## **Generation Failure**

The three types of generation considered in Chapter 4 are diesel generators, batteries, and solar panels. For diesel generators and batteries, their rates of failure can be extracted from benchmark equipment catalogs because it is assumed that they are easily stored in structures (e.g., concrete) that can resist high winds from hurricanes and storms. As for solar panels, their exposure to the open air can be problematic if not removed and stored during the event. For stand-alone systems, the number of installed solar panels are easily manageable since they are serving only one load. Therefore it is also assumed that the users will take precautions in advance to secure the panels as weather forecast provides alerts for hurricanes.

---

<sup>3</sup>Secondary cables and branches are considered to have the same rate of failure

### 5.3.3 Node Reliability

A Steiner tree seldom yields a reliable network, this is because radial configurations are the least reliable ones, but they are the cheapest. Starting with a Steiner tree, load nodes are labeled unreliable if the multiplication of the equipment upstream falls below the accepted threshold. The set threshold is also an external input subject to policy debates and certainly impacts the output of the critical distribution network.

As previously stated reliability of an equipment is  $\phi = 1 - \alpha$  where  $\alpha = \frac{\lambda(1)}{365}$ . In a radial network, load nodes reliability includes generation, substation, transformer, primary and secondary cables, and joints. Y-joints are assumed to be present at Steiner vertices, and switches are used in the presence of cycles in the network.

$$\Phi_n = \prod_i \phi_i \quad (5.3)$$

In the presence of cycles<sup>4</sup> the radial components are multiplied using equation 5.4, however the two paths of the cycle are treated separately to find their respective reliability  $\phi$ . The rate of failure  $\alpha$  of the paths are multiplied, the one's compliment of the result is then the reliability of the entire cycle.

$$\Phi_n = \prod_i \left( \phi_i * (1 - \prod_p \alpha_p) \right) \quad (5.4)$$

If a node has N cycle connecting it to its generation, then there are 2N paths. If two nodes are in a cycle, it said that they meet the N-1 safety criteria. N-1 is a net minimum reliability criterion meaning the system is planned such that for a fault on the cycle the system can operate reliably because contingency for one event is accounted for through the alternate route a cycle provides.

---

<sup>4</sup>A cycle is defined as a path of edges where a node is reachable from itself

## 5.4 Reliability

The reliability of a critical load has been associated with the compounding of the rates of failures of all the equipment required to supply power. An external threshold defines whether a load receives reliable supply or not. A tree such as the Steiner tree will have degrading node reliability as the tree expands and hence, the problem of how to improve the reliability of the critical loads if they do not meet the threshold.

Areas with existing distribution networks that have primary and alternative feeders such as selective distribution, primary loop, and spot networks benefit from increased reliability. These typical configurations rely on a primary feeder that starts at an MV/LV bus bar and an alternative feeder following the same path in case a fault occurs on the primary feeder the secondary ensures continuity of supply through the configuration of switches and branch cables. Electing to harden the primary and alternate feeders that supply the critical loads may initially appear to be the trivial solution. However, when a hurricane or a storm hits an area, it is unlikely that the primary cable gets damaged while the secondary does not if they go along the same path (which they often do) or vice-versa. Thus, ensuring a level of reliability to the critical loads requires more than typical primary and alternate distribution network.

Improving the reliability of the microgrid is then associated with identifying critical lines from the Steiner tree problem and additional alternative routes reaching the critical loads using the existing infrastructure. Hardening other lines to the Steiner tree may not always be the best option taking into consideration impact on the overall territory, power flow, and cost. Thus, decentralization of generation within the microgrid to reduce the series elements that reach the critical load may be a better option given all the considerations above.

Two approaches present themselves that can be considered when hardening a network: top-down approach of hardening more lines that create cycles in the network and bottom-up approach of relocating and re-sizing generation in the microgrid or microgrid cluster. It is helpful to understand these approaches using the simplified abstract examples presented below.

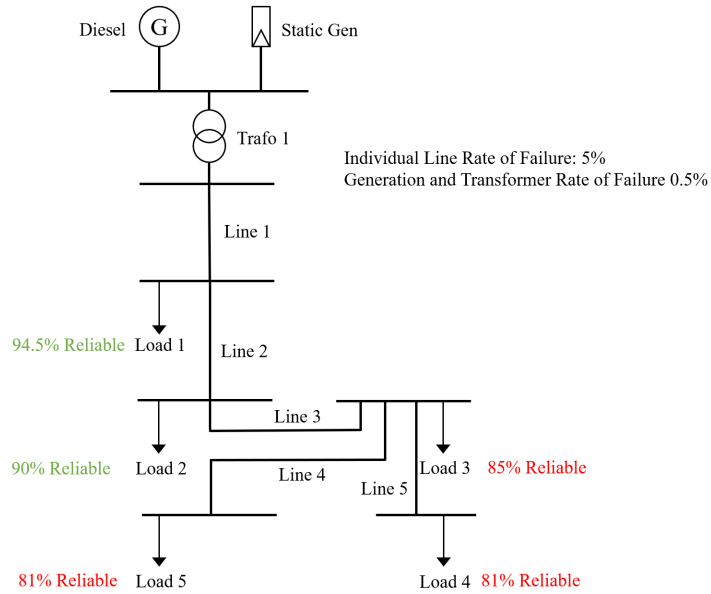


Figure 5-7: Sample network

As seen in figure 5-7, the Steiner tree solution is the radial connecting generation to all critical loads in the microgrid as developed in chapter 3. Chapter 4 sizes the generation node labeled "G", and as discussed, each equipment has a rate of failure associated with them. An algorithm finds feasible reinforcements to the radial network by identifying all the reinforcements that have a positive impact on the unreliable nodes. The search algorithm randomly lists all the top-down and bottom-up options that are technically feasible, have a positive effect on the unreliable nodes.

### 5.4.1 Top-Down Approach

Figure 5-8 shows one top-down option of adding a new line from upstream to the unreliable node to grant that node an alternate supply route. The lines are extended from upstream since that is where the microgrid or microgrid cluster generation is located. Another top-down option may be extending the new wire to the generation. Obviously this will have a more significant impact on the network since the cycle creates is more inclusive. Top-down options that do not convert unreliable nodes to reliable ones (as in taking the level of reliability at the node above the set threshold) are not considered since the cost heavily outweighs the benefit. Lines are run along

the same path as an existing critical line in the Steiner tree are not considered, a high majority of the edges along the path of the new line must be novel, after many iterations the threshold of existing edges has been empirically set to 30%. Moreover, at least 70% of the weighted edges forming the path being considered must be new, and this parameter is set to ensure sparsity of the network to minimize the impact of a random event.

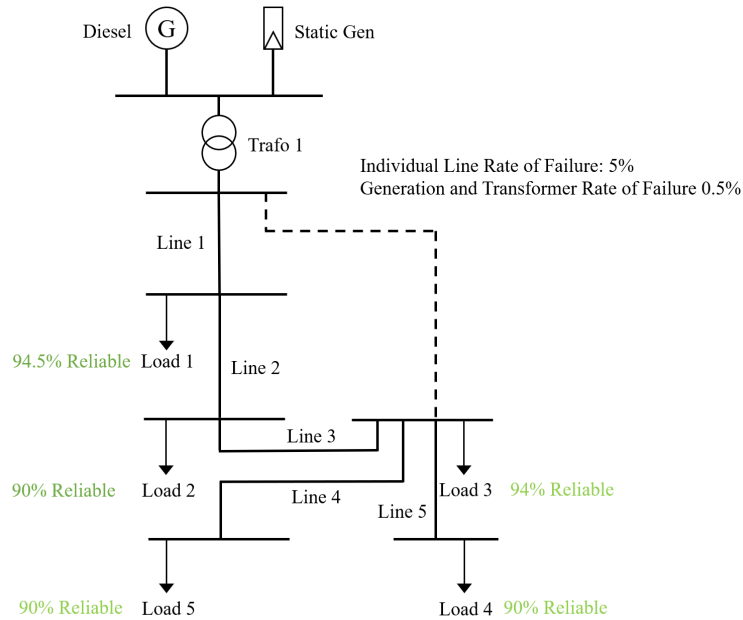


Figure 5-8: Top down reliability approach for the sample network from figure 5-7

### 5.4.2 Bottom-Up Approach

Figure 5-9 shows one bottom-up option of segmenting and distributing the generation of the microgrid. If a node is found to be unreliable, this approach presents the possibility of resizing the central generation and relocating a portion to meet the downstream demand. This will have an impact on the nodes downstream since that everything downstream of an unreliable node is unreliable. As presented in figure 5-9 a cost savings strategy of eliminating the upstream line may permanently segment the microgrid, this will impact the clustering at MV level. It can also be argued that while the apparent cost of generation decreases, the overall cost of the cluster can increase

because of excessive economies of scale. Abandoning the line and re-segmentation or decentralization of the microgrid generation can be further analyzed on a case by case basis. Further decentralization without removal of the cable, the microgrid energy resources will require more sophisticated power electronics and power flow. This research is a static study that does not develop the dynamics, but such overheads must be accounted for.

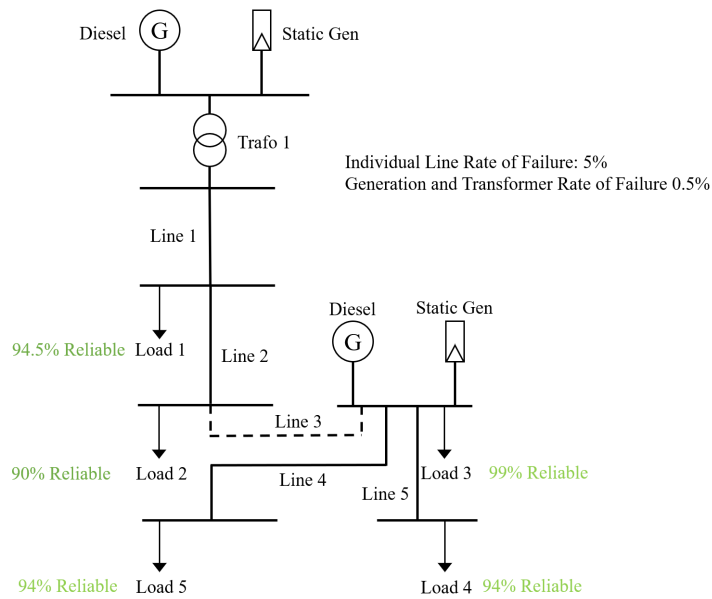


Figure 5-9: Bottom up reliability approach for the sample network from figure 5-7

## 5.5 Multi-objective Optimization (MOO)

The previous section identifies all feasible options that improve the reliability of a given distribution network. Each option (top-down or bottom-up) has a positive impact on the grid and therefore, carries attributes. Multi-objective optimization is introduced to choose an optimal or sub-optimal solution for the broad set of options made available.

The general multi-objective optimization is posed as follows:



$$\text{Min}_x F(x) = [F_1(x), F_2(x), \dots, F_k(x)] \quad (5.5)$$

$$\text{s.t.} : g_j(x) \leq 0; j = 1, 2, \dots, m \quad (5.6)$$

Where  $k$  is the number of objective functions and  $m$  is the number of inequality constraints. Pareto optimality is defined at a point where it is not possible to move in any direction that improves at least one objective function without lessening any other objective function [15]. In MOO, this often yields a Pareto optimal set of multiple Pareto points as highlighted in figure 5-10.

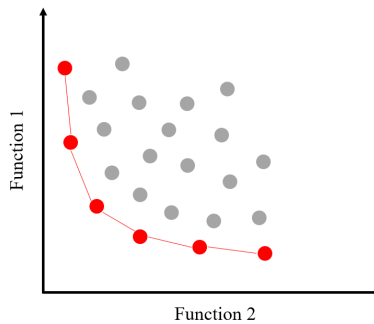


Figure 5-10: 2 Dimensional Pareto Optimal Set

Therefore, *a priori preference* must be indicated to choose a single point. The weighted sum method is a linear solution that entails selecting scalar weights to compose a tangent to the set so that a single point can be chosen.

$$U = \sum_i 1^k w_i F_i(x) \quad (5.7)$$

The signs of the weights can be manipulated in case certain objectives need to be minimized while others maximized.

### 5.5.1 Priority List

Each option from the top-down and bottom-up approaches in section 5.4 will have a cost, node impact, and demand impact associated with it. In the top-down approach, the cost of hardening the new line in USD per kilometers and at least two switches cost at the start and end of the cycle that the line has created. In the bottom-up approach, the cost includes the installation of generation sized to the downstream load by interpolating from the look-up table built in section 4.5.2 and a deduction of the cost of hardening the omitted line from the Steiner tree. Node impact is defined by the number of nodes that become reliable using the option and demand impact is the kW amount that becomes reliable.

A multi-objective optimization problem [17] is presented, with three attributes:

- Cost of option (US)
- Number of impacted load nodes (Integer)
- Amount of impacted demand (kW)

Mapping the attributes on a three-dimensional plot illustrates the weights of each decision. Any option located on the Pareto optimal set is defined as a sub-optimal solution. The Pareto optimal set is determined by cost-minimization, node impact maximization, and demand impact maximization. When multiple decisions are located on the Pareto optimal set, the weighted sum is a subjective method that converges to a single solution depending on the inputted weights of the sum. Normalization of the attribute scales can simplify the rationale of choosing a weighted sum.

Once the optimization is completed and a set is identified, a list is created that prioritizes options of all Pareto Sets (from most to least optimal). This simplifies the process of identifying multiple options without the need to optimize various times. After each choice selection, unfeasible options are filtered out, and the *priority list* has a new top choice to select from.

### 5.5.2 Case Results

These case results present two different network topologies: urban and rural. This example uses equal weights for the weighted sum linear equation 5.7. Red stars are critical loads, green triangles are MV/LV substations, black triangles are energy sources, red lines are LV primary distributions and blue lines are MV voltage.

#### Urban

Solution of Old San Juan LV network using two options from the Priority List.



Figure 5-11: Result LV and MV network of reliability model for Old San Juan

Three dimensional representation of all feasible top-down and bottom options for Old San Juan.

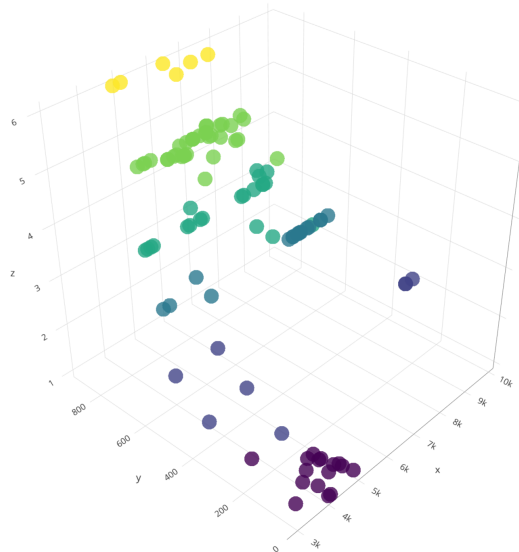


Figure 5-12: Plot of 110 options of Old San Juan

## Rural

Solution of Orocovis LV network using four options from the Priority List.

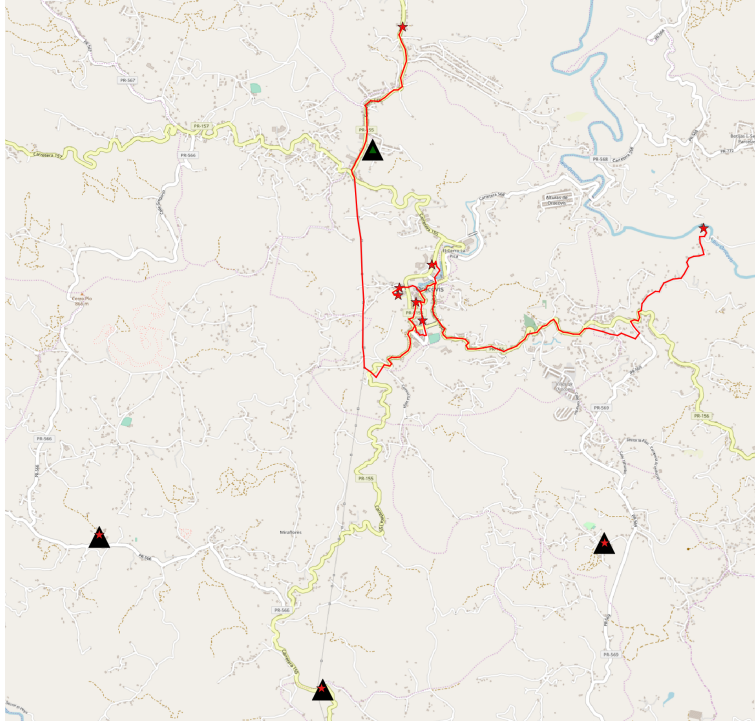


Figure 5-13: Result LV and MV network of reliability model for Orocovis

The figures 5-11 and 5-13 highlight the difference in top-down versus bottom-up reinforcement. In meshed networks the sub-optimal solution that creates cycles in the network tends to be preferred as presented in the Old San Juan case. In Rural areas where the network is mainly radial the list is limited to generation relocation options.

# Chapter 6

## Network Hardening

### 6.1 Overview of Network Hardening

The previous chapters have been concerned with the critical operation, which is defined by a reliable method of powering the critical infrastructure post-natural disaster. Regardless of the status of the main grid, the critical infrastructure must have a reliable electricity supply and so far this thesis has explored how the deployment of microgrids and their clustering at distribution level can improve resiliency and secure an acceptably reliable supply of electricity to loads that are critical to the area as defined in chapter 2. While the previous chapters have discussed the critical mode of operation, this chapter evaluates normal operation mode and how the deployment of distributed energy resources from the critical mode impacts the normal operation mode.

However, such decentralization must be accounted for in normal operation. While hurricanes are increasingly likely to hit a particular area, they remain random events that cannot be forecasted more than several weeks in advance. Thus, the question of hardening the main grid instead of deploying microgrids is necessary to address and if critical microgrids are deployed, what should be the operation mode of the non-critical demand in the medium term. The questions raised are both technical and policy-related, it is essential to define a policy framework to design solutions that meet the mechanical constraints. Given the recent history of catastrophic emergency

response on the Island of Puerto Rico, it is firmly assumed that distributed energy resources for critical loads must operate entirely in the off-grid mode for a considerable amount of time mainly dictated by the designed size of the stores. Therefore, the investment in the critical microgrids must be considered a sunk cost that should not be evaluated in normal operation analysis.

This section looks at the entire demand of the MV/LV substations to evaluate whether the territory should operate entirely off-grid and neglect any grid connections that reach it or improving the resiliency of the transmission<sup>1</sup> for grid connection while taking advantage of the abundant renewable energy sources from the critical microgrids. It can be inferred that substations in rural areas where the high-voltage network must be extensively extended to reach them tend to become completely off-grid. However, larger clusters can be formed to justify the cost of upstream hardening. This will result in reshaping the existing high-voltage and transmission network by identifying important lines that are needed in the medium to long terms to maintain an acceptable level of reliability post-natural disaster.

## 6.2 Upstream Hardening Decision

In rural electrification, a decision must be made on whether to extend the existing grid or design an off-grid solution via either mini-grids or stand-alone systems for smaller loads. Extending the grid includes the cost of reinforcement, expansion of the transmission network, and centralized generation units that can be quantified in volumetric units of USD per kWh. The grid will have an input level of reliability based on its status, and the off-grid solutions will have a calculated level of reliability based on demand size and resources. REM calls RNM Greenfield to reproduce the existing grid and RNM Brownfield to calculate the reinforcements needed when introducing the potential demand REM generates, the Upstream Network Reinforcement Process (UNR) is described further here [8].

---

<sup>1</sup>Transmission is defined as the transmission and high voltage networks that connect generating stations to the distribution network.

A similar process is proposed while taking into consideration the difference in the application. It is important to note that UNR is concerned with reinforcement, which is defined as the transmission and generation expansion needed to accommodate additional demand on the grid. This is not the concern of this research because the hypotheses are that the electrical grid has been already sized for the existing peak demand where all the loads considered all connected, hence expansion planning is not an objective. However, hardening can be looked at similarly, transmission lines can be identified as important to deliver power from the generation units to the distribution network using a cost allocation method developed later. Once the lines are identified and allocated to a distribution cluster, the grid-connection cost of that cluster can be calculated and compared to the off-grid cost to make a decision the same way REM does (i.e., cost minimization basis).

### **6.2.1 Off-Grid Cost**

Considering the clusters produced in chapter 5 at distribution level for the critical infrastructure, it can be inferred that higher demand in the cluster encourages the medium voltage hardening due to generation economies of scale as well as the stronger justification of hardening cost since the majority of the cost of an underground line is due to the hardening process rather than the size of the line.

Using those clusters and applying microgrid designs of chapter 4 on both critical and non-critical demands produces the completely off-grid solution for the territory being studied. The levelized cost of energy is the volumetric unit used for off-grid generation cost presented in chapter 4 in USD per kWh.

### **6.2.2 Grid Connection Cost**

Grid connection considers the historic levelized cost of energy of the generation units. The identified demand is the total demand of the cluster (both critical and non-critical) but with the deduction of the portion of demand that can be satisfied by the renewable sources (i.e., solar and batteries) of the critical microgrids.

## 6.3 Cost Allocation

An assessment of the need for the transmission network is required due to the drastic changes proposed at the distribution level. The input reliability level an area requires influences the decision between grid connection and off-grid solutions in normal operation mode. Main grid reliability parameters can be changed to produce different results and compare solutions to adopt a sub-optimal policy with cost awareness.

It is common to see a high LCOE for microgrids, and chapter 4 paints a deceptive picture of deploying microgrids at a very low LCOE (which enables the justification of the hardening cost of the distribution network). However, the number of solar panels is limited, and the demand is now expanded to regular operation, which increases drastically. This will require more diesel generators and batteries, the former has high variable cost, and the latter has a relatively short life, which leads to a high LCOE. However, is the LCOE of the off-grid solution high enough to justify the cost of upstream hardening?

A cost allocation method is proposed to weigh the grid-connected cost of energy, including USD per kWh upstream hardening and off-grid cost of energy:

1. Identify pool of microgrids and microgrid clusters
2. Aggregate microgrid clusters into single MV/LV substation closest to HV/MV substation
3. Identify MV lines connecting aggregated MG clusters to HV/MV substations
4. Evaluate MV connection to HV/MV substations
5. Identify HV lines connecting aggregated demand at HV/MV substation
6. Evaluate HV connection to transmission substation
7. Identify transmission lines connecting aggregate demand at transmission substation to generation
8. Evaluate transmission connection to generation units



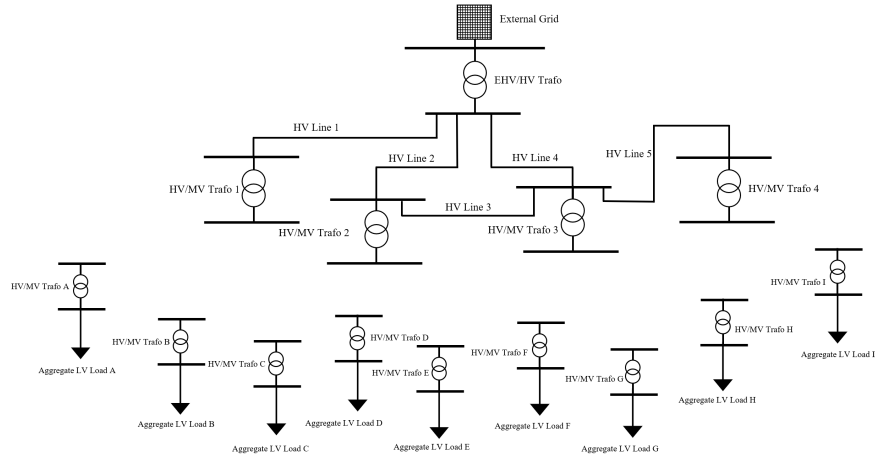


Figure 6-1: Cost Allocation Example Network

The medium voltage network is generally radial but connection to multiple HV/MV substations is possible. An initial k-mean clustering of MV/LV substations with HV/MV substations as centers. Clustering based on the nearest neighbor may not always yield the best solution and therefore reallocation of MV/LV substations that can be connected to multiple HV/MV substations within reasonable distance are explored. This results in several combinations of the pool of microgrid clusters. Additionally, if multiple microgrids are connected their demand is aggregated into a single node that is directly connected to a HV/MV substation via a high voltage line.

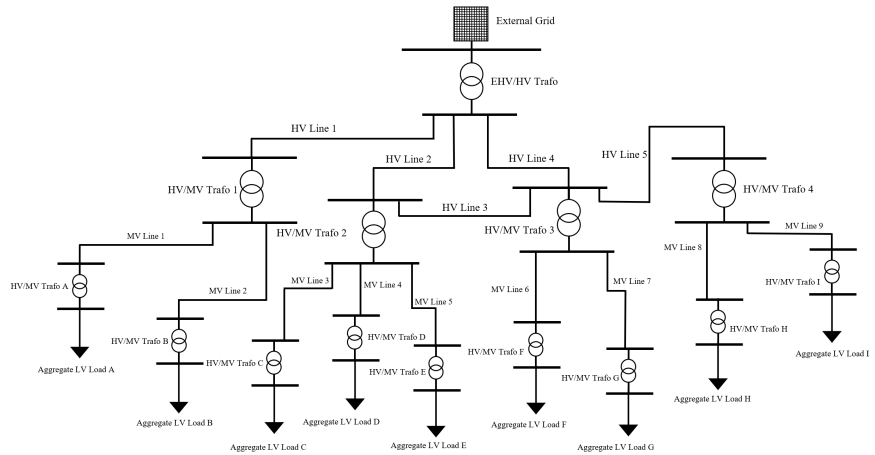


Figure 6-2: Cost Allocation Example: Combination 1

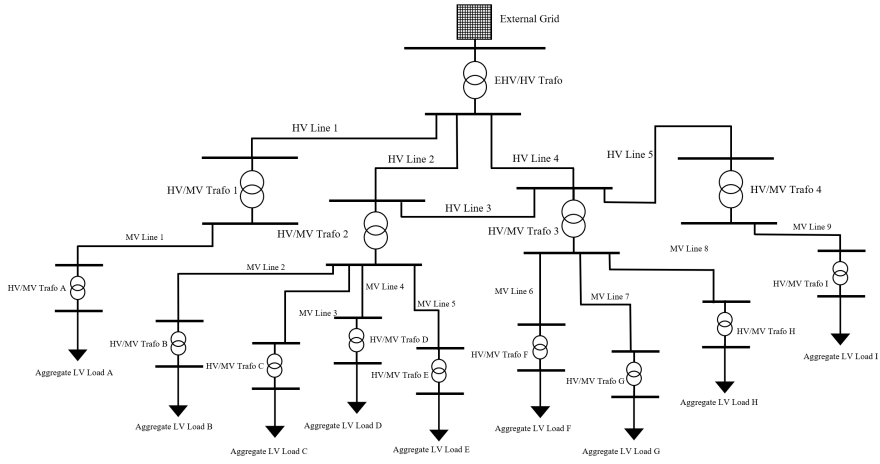


Figure 6-3: Cost Allocation Example: Combination 2

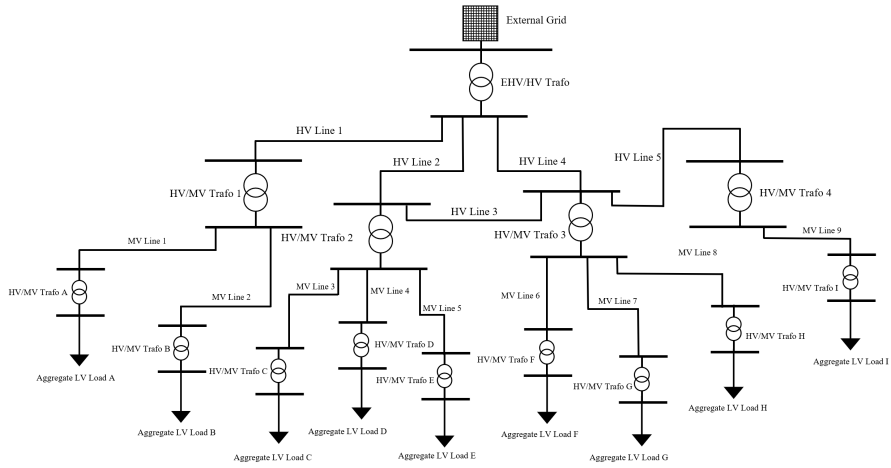


Figure 6-4: Cost Allocation Example: Combination 3

### 6.3.1 Decision Tree Algorithm: Case Example

#### MV Aggregation

An algorithm is a bottom-up approach starting at the aggregated MV/LV substations that are directly connected to HV/MV substations via medium voltage lines. Connection lines that are too expensive to harden are ignored, making it obvious to go the off-grid route as depicted below. The cost terms for grid connection are centralized generation cost, hardening cost, and network losses. The cost terms for off-grid are microgrid generation cost, savings upstream due to disconnection and microgrid losses. Combination 1 and 3 are further developed below:

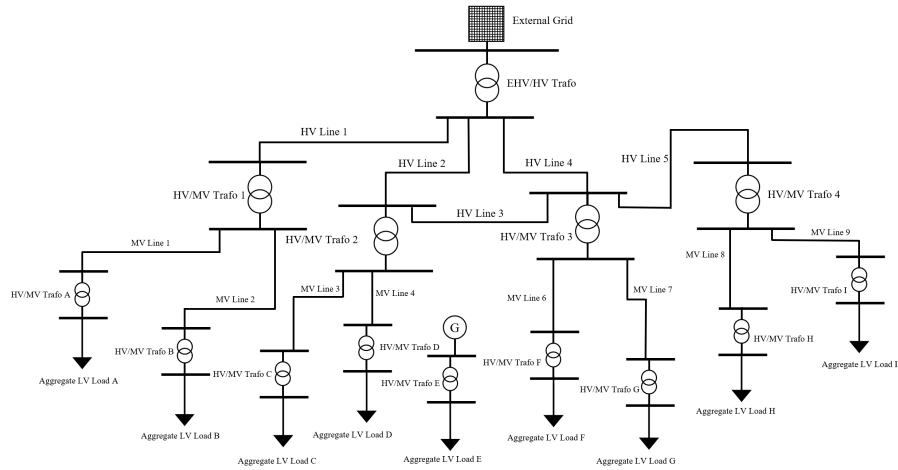


Figure 6-5: Cost Allocation Example: Combination 1 Off-grid MV Filtering

No solution is favored yet, whether it is the one with most grid-connected MV/LV substation or the most off-grid ones.

#### MV Folding

After finding which lines are worth maintaining, the HV/MV substation will have a group of medium voltage aggregated loads as children. The demand can be aggregated at the HV/MV substation, i.e., for Combination 3 HV1 will have the demand of A and B, HV2 will have C and D, HV3 will have F, G and H and HV4 will have I (Note that E is not considered anymore).

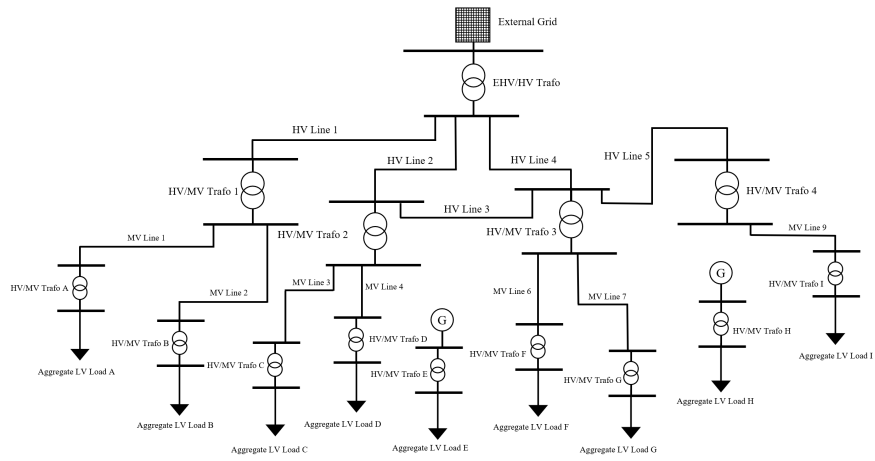


Figure 6-6: Cost Allocation Example: Combination 3 Off-grid MV Filtering

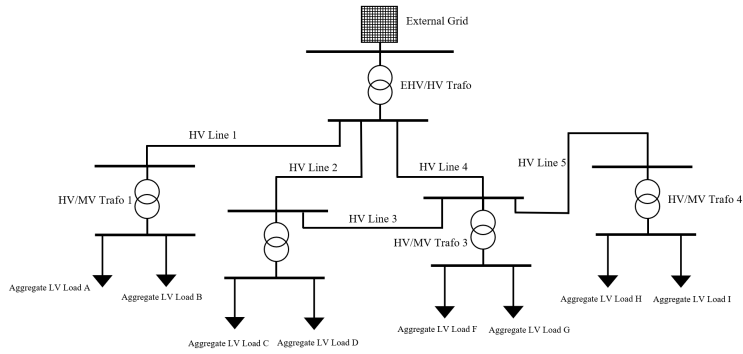


Figure 6-7: Cost Allocation Example: Combination 1 Off-grid MV Folding

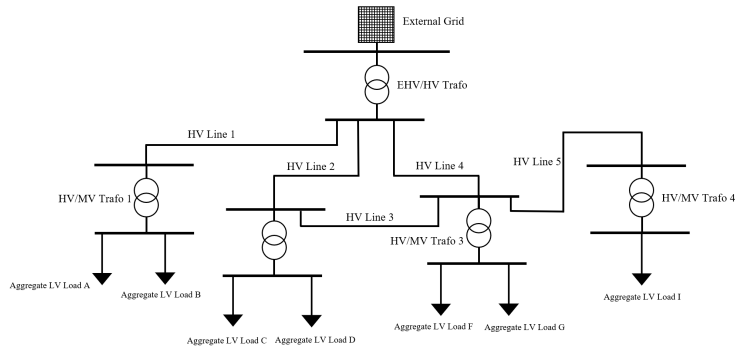


Figure 6-8: Cost Allocation Example: Combination 3 Off-grid MV Folding

$Gen()$  function is defined as the main grid cost of generation as a function of demand.  $H()$  function is defined as the hardening cost at the designated voltage level as a function of length.  $MG()$  function is defined as the microgrid cost of generation.

## MV Decision

At each HV/MV substation, an inequality is presented that will lead to the medium voltage level decision. If the cost of generation from the main grid with the total hardening cost of the medium voltage network under the HV/MV substation is lower than the microgrid cost of the generation, then it is worthwhile investing in hardening the medium voltage network. If the below inequality holds then the medium voltage lines under the HV/MV substation of interest is adopted and labeled as a priority, and the upstream search continues at the HV/MV substation of interest. Otherwise, the solution will break into microgrids and the medium voltage network will be ignored<sup>2</sup>:

$$Gen(x + y) + H(l_{MV}) \leq MG(x) + MG(y) \quad (6.1)$$

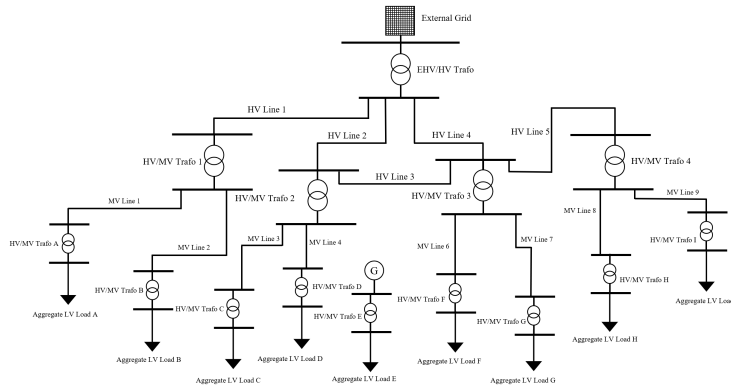


Figure 6-9: Cost Allocation Example: Combination 1 Off-grid MV Decision

## HV Minimum Spanning Tree

If no MV/LV substations are connected to an HV/MV substation then the line reaching the latter substation can be ignored if it is not shared with any other substation

<sup>2</sup>This case example does not highlight savings cost and reliability of generation penalty

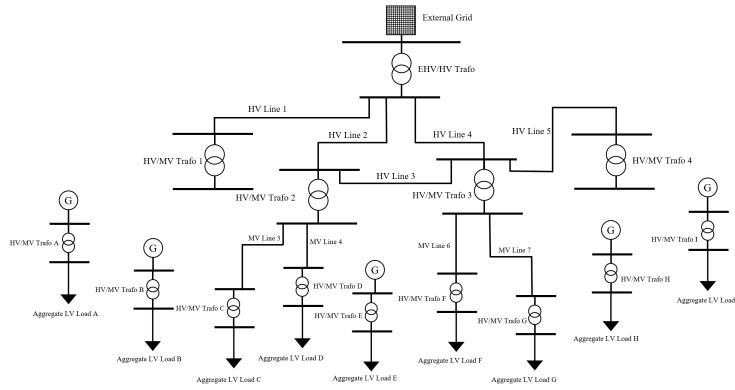


Figure 6-10: Cost Allocation Example: Combination 3 Off-grid MV Decision

being considered, such as  $HV\_L\_1$  in figure 6-10. Since the high voltage network is considerably meshed finding a minimum spanning tree yields the minimum cost solution. The minimum spanning tree must interconnect HV/MV substations, generation at high voltage and transmission substations. When the latter two do not exist a high voltage interconnection of the substations for a defined zone is enough to evaluate the high voltage lines.

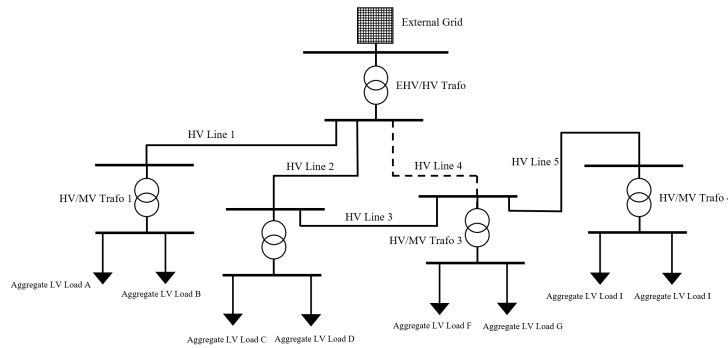


Figure 6-11: Cost Allocation Example: Combination 1 Off-grid HV MSP

Different minimum spanning trees are shown in figures 6-11 and 6-12 are for illustration purposes and are not representative of a single network configuration.

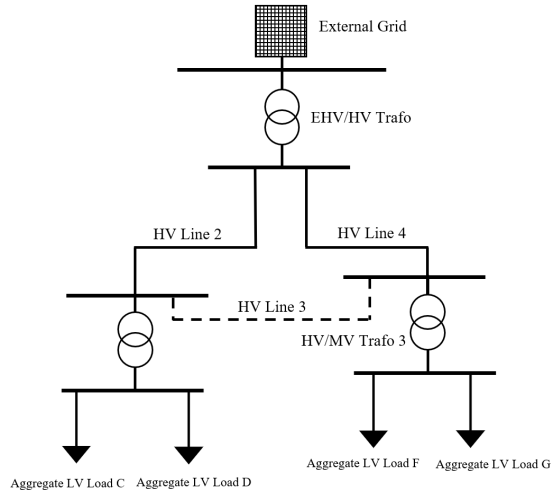


Figure 6-12: Cost Allocation Example: Combination 3 Off-grid HV MSP

## HV Solution

It is evident that more connection justifies the cost of maintaining a line, and therefore the cost of maintaining a high voltage line along with all the costs downstream of the HV/LV substations that have been justified by the MV Decision also need to outweigh the cost of the off-grid solution. If a generation or a transmission is available in the defined zone, then that's where the aggregation of the HV/LV substation takes place. Otherwise, the HV substations are just aggregated as a single node for further connection at high voltage or transmission with another zone.

Certain lines are shared by multiple HV/MV substations and therefore, the cost of hardening that individual line is compared to the off-grid alternative of all the affected medium voltage nodes. Using the same equation 6.1, the result will indicate whether it is better to connect upstream or spread out the medium voltage stations as a microgrid.

### 6.3.2 Solution

The cost allocation algorithm evaluates medium voltage lines and HV/MV substations. Usually, there are multiple MV/LV substations downstream of the substation that is directly connected to the high voltage network, and therefore the same "tree

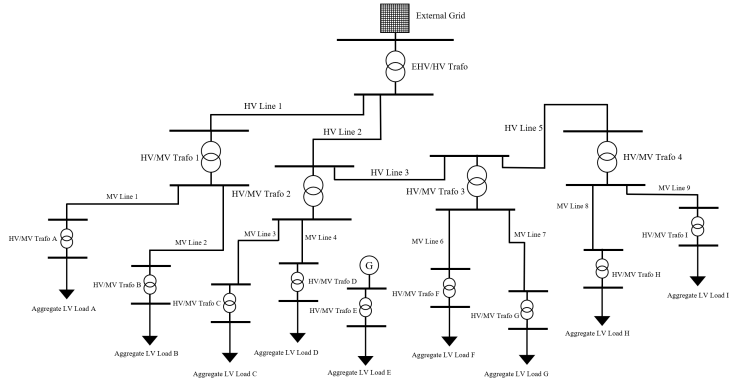


Figure 6-13: Cost Allocation Example: Combination 1 Off-grid HV Solution

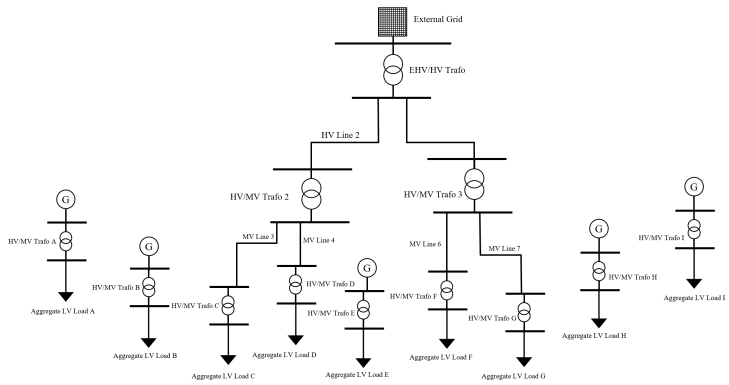


Figure 6-14: Cost Allocation Example: Combination 3 Off-grid HV Solution



folding" process can be applied to reach a single node that aggregates all the MV/LV substation downstream of the HV/MV substation as a single connection. It is part of the algorithm's architecture to pro-rate line cost to the amount of demand that is being utilized, meaning the line most downstream will have the high USD per kW cost and the one most upstream will have the lowest USD per kW cost since more demand is being aggregated as the tree is being folded.

Overall, the solution starts by considering a grid-connected network, then evaluates the line connection in a bottom-up fashion. The cost of maintaining a line is only justified if the cost of branching everything downstream of that line as off-grid is higher by taking into consideration quantified reliability measures and savings in a generation.

As portrayed in the example of section 6.3.1 if a transmission substation is considered the highest point the zone being evaluated (the same applies for a generation station instead). The cost of maintaining the network downstream of that station must be cheaper than the alternative of off-grid. It can be directly inferred that there will be a minimum amount of demand needed downstream of the substation for the economies of scale of a generation with the cost of maintenance of the lines is attractive. This depends on the line configuration as well as the amount of connected demand.

### **6.3.3 Top-down observation**

The cost allocation approach is the most inclusive since the initial state is complete grid-extension. A particular case may arise that the cost of maintaining a high voltage line is not justified due to the downstream demand not being large enough because much medium voltage lines have been ignored and the stations are operating off-grid. If the cost of maintaining a medium voltage line is not smaller than the off-grid solution, then the marginal benefit of considering that line further upstream is negative since the maintenance cost increases with voltage level.

It may be argued that less demand from the main grid reduces congestion and thus reducing the cost of energy, or more demand increase economies of scale, which

also reduces the cost of energy. With enough data, these cost savings can be modeled as linear constraint functions, and the cost allocation algorithm can be optimized with a minimum cost objective function.

### 6.3.4 Reliability Metrics

The dotted high voltage lines in figures 6-11 and 6-12 are lines that are not part of the tree solutions since they create cycles in the high voltage network. However, these lines are important to improve the reliability level of the electrical network. This is similar to the Top-Down Approach of section 5.4.1. This also calls for the usage of multi-objective decision making with the cost of the option, impacted demand, and reliability level attributes. Similar to section 5.5.1, a Pareto optimal set yields a solution given the weights of the attributes.

Cost, impacted demand, and reliability calculations have been developed in Chapter 5; however, since this chapter is concerned with connection to the grid, the reliability of the external grid must be considered. Grid-connected energy sources have different reliability levels and may not be available post-hurricane, such as windmills and solar photovoltaic parks.

## 6.4 Case Study

Figure 5-5 highlights the identified microgrid territories PREPA has identified part of their resiliency plan. To present a realistic case for Puerto Rico, the six states surrounding the state of San Juan are taken under consideration: Toa Baja, Cataño, Bayamón, Guaynabo, Trujillo Alto, Carolina. These seven states are divided into 3 microgrids, figure 6-15 shows the geographic location of the MV/LV transformers of each microgrid territory.

Using the Steiner Tree Algorithm developed in Chapter 3, the MV tree network is presented in figure 6-16.

The MV network is then segmented, and the MV/LV stations are either branched away from the grid as microgrids or connected to the nearest HV/MV station.

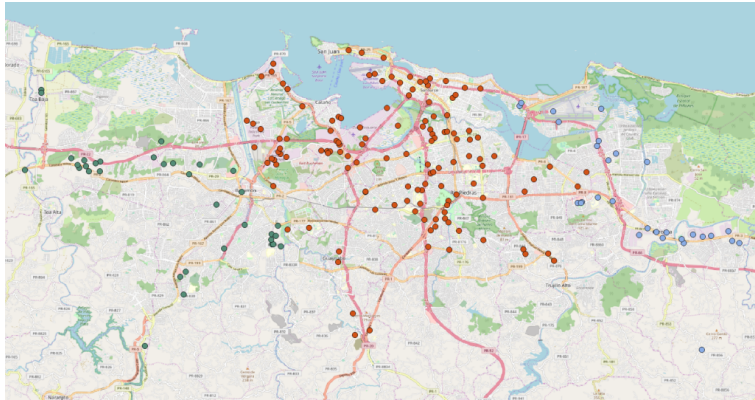


Figure 6-15: MV/LV Transformer location

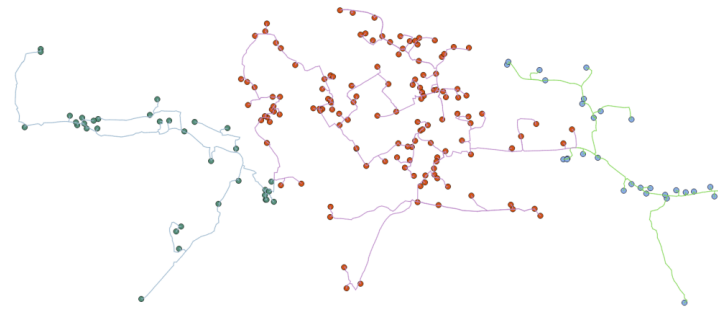


Figure 6-16: MV Steiner Tree

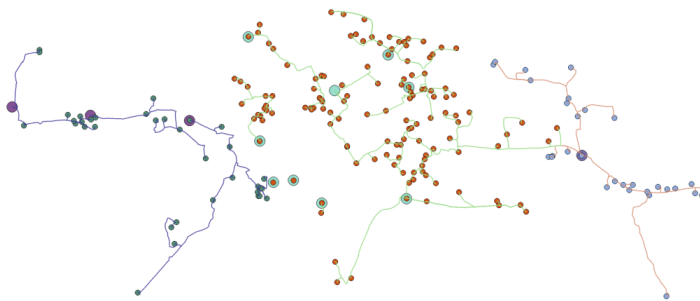


Figure 6-17: MV Network post segmentation

The HV network connecting the HV/MV stations is presented in figure 6-17, where the red lines are HV cables connecting HV/MV stations within a territory, the blue lines are cables interconnecting territories and the green lines are secondary lines creating meshes in the HV networks which will be used to improve the reliability of the system in a later step.

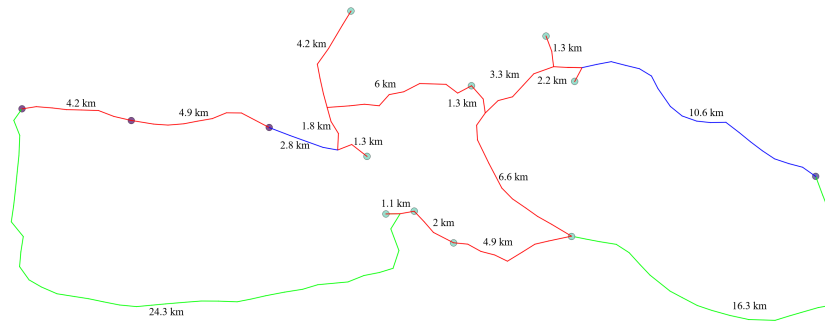


Figure 6-18: Line lengths of HV network

While figure 6-19 shows the aggregated and allocated LV estimated demand to the HV/MV stations totalling 3.95 billion kWh per year.

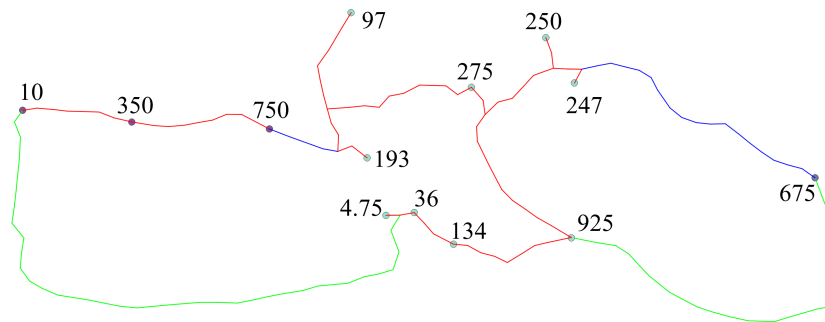


Figure 6-19: Aggregated estimated demand at HV/MV stations in Millions of kilowatt-hours

It now a cost comparison to decide whether to switch to off-grid or to stay connected to the main grid. Repeating this exercise and comparing total costs for different projects as the decision tree expands yield a conservative solution. Figure 6-20 illustrates one of many possible solutions for the state of San Juan and its neighboring states.

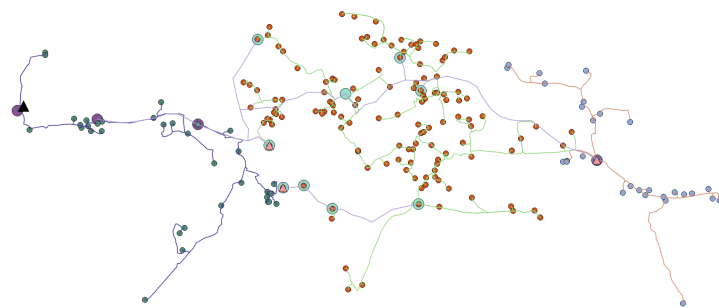


Figure 6-20: Solution for the San Juan and neighboring states

THIS PAGE INTENTIONALLY LEFT BLANK

# Chapter 7

## Summary, Discussion, and Conclusions

In summary, the research carried out in this thesis is concerned with the static representation of the electrical grid and improvement of its resiliency through the deployment of microgrids as well as hardening of the existing network. Chapter 2 presented a geographic information system based method to represent the electric grid using polygon to centerline conversion through triangulation methods. Chapter 3 identified the critical infrastructure and network essential to the operation of a populated area. Chapter 4 developed a linear programming optimization tool to size microgrid generation while taking into consideration the unique circumstances post-natural disaster. Chapter 5 introduced resiliency metrics needed to maintain a satisfactory level of reliability through multi-objective decision making. While chapter 5 addressed resiliency at the low voltage distribution level, chapter 6 considered the hardening of the medium and high voltage networks through decision trees and capital budgeting tools.

In summary, only the critical infrastructure is considered for resiliency planning. The philosophy adopted is that, regardless of the status of the grid, the critical infrastructure must be supplied with energy and therefore the identification of the critical lines and the deployment of microgrids from chapters 3 and 4 are used.

Nevertheless, a clear path to recovery for the overall grid must minimize grid dam-

age, and outages. Therefore, chapters 5 and 6 develop tools to improve the reliability of the network at primary distribution as well as medium and high voltages. Such planning considers two options: grid connection and off-grid (microgrid). The microgrid design tool from chapter 4 is used again over larger territories after clustering neighborhoods together.

This research has primarily concerned itself with GIS-based models using optimization tools for power systems. However, the application to some cases on Puerto Rico raise some issues worth discussing. Constrained by technical feasibility, the cost of energy primarily dominates the optimal grid structure. The initial investment needed to harden the existing grid does not affect the solution significantly. Even though it is a large amount of money to be invested, it can still be easily recovered in the long term, given an adequate tariff design. The main decision variable for the connection type output is the cost of energy, be it main grid or microgrid.

The scope of this research is limited to the development of useful tools that can provide technical insight on where to deploy microgrids through cost minimization and reliability constraints to improve the resiliency of a network. As previously disclaimed, the results presented here are not intended to be implementable recommendations for policymakers and utility planners, as the data that was used is either gathered from open sources or estimated.

## 7.1 Future Work

It is essential to take into consideration the impact of integrating distributed energy resources on the main grid and how these resources impact power flow and line loading when prioritizing lines for maintenance and investments. Either off-grid or grid-connected solutions have been considered for regular operation with little attention to the sunk cost of distributed energy resources deployed for a critical operation. While the solution in many cases is islanded microgrids, to minimize dependability hybrid systems should exist. A hybrid system is defined as a network that is primarily powered by local energy sources but does depend on the external grid to a certain



extent. The pressure of resorting to the main grid is reduced, and the grid structure must also be adapted.

The work developed in this thesis is limited to distribution at all voltage levels, where, for the most part, meshed networks were decomposed, and a radial network was extracted as the primarily used one. Expanding the research into transmission gives a clearer picture regarding the investment needed to maintain the grid, thus be able to locate microgrid sites better. Transmission expansion planning and reinforcement serve as a fitting complement to the distribution planning models developed here.

THIS PAGE INTENTIONALLY LEFT BLANK

# Appendix A

## Tables

Table A.1: Diesel generator investment cost bracket

Generator Size (kW)	Investment Cost (USD)	Investment Cost (USD per kW)
5	3,200	640
10	4,643	464.3
20	6,737	336.85
40	9,776	244.4
60	12,154	202.57
80	16,080	201
100	20,000	200
125	25,000	200
150	30,000	200
175	35,000	200
200	40,000	200
250	50,000	200
300	60,000	200
350	70,000	200
400	80,000	200
500	100,000	200
750	150,000	200
1000	200,000	200

Table A.2: Generation facilities of Puerto Rico

Name	Capacity (MW)	Type
AES Ilumina	24	Solar
AES Puerto Rico	454	Coal
Aguirre Combined Cycle	592	Heavy Fuel Oil
Aguirre Thermoelectric	900	Diesel Oil
Cambalache	247	Diesel Oil
Caonillas 1	18	Hydro
Caonillas 2	3.6	Hydro
Costa Sur Power	990	Heavy Fuel Oil
Dos Bocas	15	Hydro
EcoElectrica	540	Natural Gas
Garzas	12.24	Hydro
Jobos	42	Heavy Fuel Oil
Mayaguez	220	Heavy Fuel Oil
Naranjito	No Information	Hydro
Oriana Solar Park	58	Solar
Palo Seco Power Plant	602	Heavy Fuel Oil
Patillas	1.4	Hydro
Punta Lima	26	Wind
Rio Blanco	5	Hydro
Salinas Solar Park	16	Solar
San Fermin Solar Farm	27	Solar
San Juan Combined Cycle	464	Diesel Oil
San Juan Thermoelectric	400	Heavy Fuel Oil
Santa Isabel Wind Farm	101	Wind
Toro Negro	10.56	Hydro
Vega Baja	42	Heavy Fuel Oil
Windmar Ponce	4.5	Solar
Yauco	29	Hydro

Table A.3: Diesel fuel transportation cost to rural territories

Tank Size (Liters)	Transportation Cost (USD per Liter)
[0; 250]	0.05
[251; 500]	0.1
[501; 750]	0.15
[751; 1000]	0.2
[1001; $\infty$ )	0.25

Table A.4: Diesel fuel transportation cost to urban territories

Tank Size (Liters)	Transportation Cost (USD per Liter)
[0; 250]	0.03
[251; 500]	0.08
[501; 750]	0.12
[751; 1000]	0.18
[1001; $\infty$ )	0.2

THIS PAGE INTENTIONALLY LEFT BLANK

# Appendix B

## Code

### B.1 Steiner Tree Algorithm

```
import networkx

M = shortest_path_net(G)
ST = steiner_tree(G, M, Terminals)

def shortest_path_net(G, weight='weight'):
    M = networkx.Graph()
    Gnodes = set(G)

    iter = networkx.all_pairs_dijkstra(G, weight=weight)
    u, (distance, path) = next(iter)

    Gnodes.remove(u)
    for v in Gnodes:
        M.add_edge(u, v, distance=distance[v], path=path[v])

    for u, (distance, path) in all_paths_iter:
```

```

    Gnodes.remove(u)
    for v in Gnodes:
        M.add_edge(u, v, distance=distance[v], path=path[v])

    return M

def steiner_tree(G, M, terminal_nodes, weight='weight'):
    H = M.subgraph(terminal_nodes)
    mst = networkx.minimum_spanning_edges(H, weight='distance')

    edges = chain.from_iterable(pairwise(d['path']) for u, v, d in mst)
    ST = G.edge_subgraph(edges)

    return ST

```

## B.2 Clustering Algorithm

```

import networkx

def split_graph(G, weight='weight', length='length', line_cost):
    edges = list(G.edges())
    e = networkx.get_edge_attributes(G, length)
    edge_length = list(e.values())
    w = list(G.nodes(data=weight))
    weight = []
    node_weights = []
    for i in w:
        if i[1] is None:
            weight.append((i[0], 0.0))
        else:

```



```

weight.append((i[0], float(i[1])))

for i in weight:
    node_weights.append(i[1])

con_comp = []
edge_split = []

Var, junction = [], []
for i in networkx.nodes(G):
    for j in networkx.all_neighbors(G, i):
        Var.append(j)
    if len(Var) > 2:
        junction.append(i)
        Var = []

for i, k in zip(edges, edge_length):

    G.remove_edge(i[0], i[1])

    edge_split.append((i[0], i[1]))
    a = list(networkx.connected_component_subgraphs(G))

    b = list(a[0].nodes())
    bw = []
    for j in b:
        bw.append(node_weights[j])
    c = list(a[1].nodes())
    cw = []
    for j in c:

```

```

        cw.append(node_weights[j])

sum_b = sum(bw)
sum_c = sum(cw)
con_comp.append((sum_b, sum_c))

G.add_edge(i[0], i[1], weight=k)

diff = []
for i in con_comp:
    diff.append(abs(i[0] - i[1]))
val = min(diff)
ind = diff.index(val)

remove = edges[ind]

return G

```

# Bibliography

- [1] Geofabrik. <https://www.geofabrik.de/>, 2018.
- [2] OpenEI. <https://openei.org/datasets/files/961/pub/>, 2018.
- [3] OpenStreetMap. <https://www.openstreetmap.com/>, 2018.
- [4] Voronoi diagram. [https://en.wikipedia.org/wiki/Voronoi\\_diagram](https://en.wikipedia.org/wiki/Voronoi_diagram), 2019.
- [5] Puerto Rico Electric Power Authority. Prepa fiscal plan march 2018. Preliminary draft, 2018.
- [6] R. E. Brown, G. Frimpong, and H. L. Willis. Failure rate modeling using equipment inspection data. *IEEE Transactions on Power Systems*, 19(2):782–787, May 2004.
- [7] Richard E. Brown. *Electric Power Distribution Reliability*. Power Engineering. CRC Press, second edition, 2009.
- [8] Turner Cotterman. Enhanced techniques to plan rural electrical networks using the reference electrification model. Master’s project, Massachusetts Institute of Technology, Institute for Data, Systems, and Society, June 2017.
- [9] Pablo Duenas-Martinez. Rnm-us input data processing from geospatial databases.
- [10] Douglas Ellman. The reference electrification model: A computer model for planning rural electricity access. Master’s project, Massachusetts Institute of Technology, Institute for Data, Systems, and Society, June 2015.
- [11] A. Golly and J. M. Turowski. Deriving principal channel metrics from bank and long-profile geometry with the r package cmgo. *Earth Surface Dynamics*, 5(3):557–570, 2017.
- [12] Aric A. Hagberg, Daniel A. Schult, and Pieter J. Swart. Exploring network structure, dynamics, and function using networkx. In Gaël Varoquaux, Travis Vaught, and Jarrod Millman, editors, *Proceedings of the 7th Python in Science Conference*, pages 11 – 15, Pasadena, CA USA, 2008.

- [13] M. Kolcun, M. Kornatka, A. Gawlak, and Z. Čonka. Benchmarking the reliability of medium-voltage lines. *Journal of Electrical Engineering*, 68:212–215, May 2017.
- [14] National Renewable Energy Laboratory. Energy snapshot: Puerto rico. Energy transition initiative: Islands.
- [15] G. Latorre-Bayona and I. J. Perez-Arriaga. Chopin, a heuristic model for long term transmission expansion planning. *IEEE Transactions on Power Systems*, 9(4):1886–1894, Nov 1994.
- [16] Vivian Li. The local reference electrification model: A comprehensive decision-making tool for the design of rural microgrids. Master’s project, Massachusetts Institute of Technology, Institute for Data, Systems, and Society, June 2016.
- [17] R. Timothy Marler and Jasbir S. Arora. The weighted sum method for multi-objective optimization: new insights. *Structural and Multidisciplinary Optimization*, 41(6):853–862, Jun 2010.
- [18] C. Mateo Domingo, T. Gomez San Roman, Á. Sanchez-Miralles, J. P. Peco Gonzalez, and A. Candela Martinez. A reference network model for large-scale distribution planning with automatic street map generation. *IEEE Transactions on Power Systems*, 26(1):190–197, Feb 2011.
- [19] Daniel Studer Kyle Benne Brent Griffith Michael Deru, Kristin Field and Paul Torcellini. U.s. department of energy commercial reference building models of the national building stock. Technical report, National Renewable Energy Laboratory, 2011.
- [20] Alicia Noriega. Energy resilience on a local level: Inclusive planning for disaster. Master’s project, Massachusetts Institute of Technology, Department of Urban Studies and Planning, June 2018.
- [21] Government of Puerto Rico. Transformation and innovation in the wake of devastation. an economic and disaster recovery plan for puerto rico. Preliminary draft for public comment, 2018.
- [22] Chotipat Pornavalai, Norio Shiratori, and Goutam Chakraborty. Neural network for optimal steiner tree computation. *Neural Processing Letters*, 3(3):139–149, Aug 1996.
- [23] Miguel Fernandez Vincent Lemort Sergio Balderrama, Walter Canedo and Sylvain Quoilin. Techno-economic optimization of isolate micro-grids including pv and li-ion batteries in the bolivian context. In Tatiana Morosuk and George Tsatsaronis, editors, *The 29th international conference on efficiency, cost, optimization, simulation and environmental impact of energy systems*, Journal of Energy Resources Technology, June 2016.